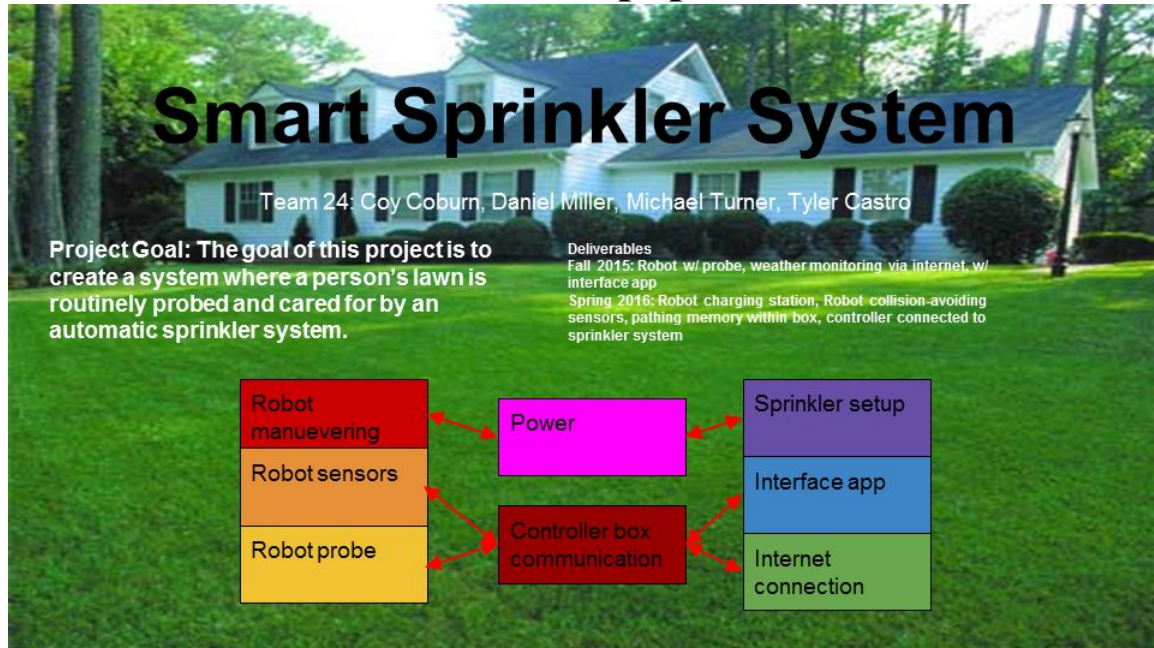


I-	White paper	pp 2
II-	Modified White Paper	pp 4
III-	Project Change	pp 17
IV-	Proposal	pp 18
V-	CDR Presentation	pp 33
VI-	Mid Term Report	pp 39
VII-	Final PPT	pp 72
VIII-	Final Report	pp 80

Please note that this first Header page is to be placed on top all requested documents from (I up to VII). Please, specify on this Header page according to each document Section the pages numbers. Page numbers have to be displayed on each document. Paging numbers start from 1 for each document.

I - White paper



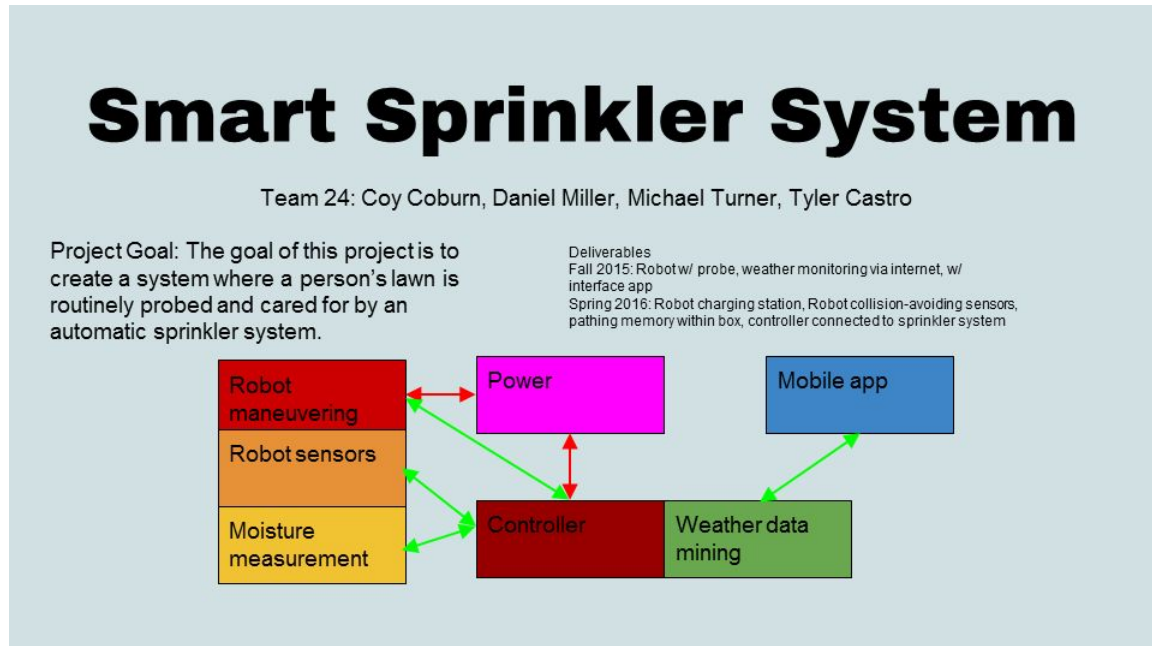
Subsystem	Primarily Responsible Team Member	Student Responsibilities/ Tasks
Power	Daniel	Prepare the necessary power supply for both the probe as well as the sprinkler system.
Controller box communication	Coy	Create a connection between the master controller with its slave connections, these include the probe, the sprinkler system, and the interface app.
Robot maneuvering	Daniel	Enhance the robot's ability to maneuver off-terrain and possess the ability to set a route for probing locations.
Robot sensing	Michael	The robot will need the functions to sense its surroundings and take necessary precautions to avoid obstacles and safely maneuver a lawn.
Robot probe	Tyler	A probe will be set to sample water moisture in multiple locations in the lawn and reset said probe.
Sprinkler setup interface	Tyler	The sprinkler system will have the functions to design and manipulate the weekly settings for lawn care with data from probe and internet.
Interface app	Coy	A mobile app will be created for a user to view sprinkler settings as well as make changes to planned watering for the week or its default.
Internet connection	Michael	The sprinkler master controller will need to connect to weather websites via internet so to plan watering settings for the upcoming week.

Team 24 Ground Penetrating Radar

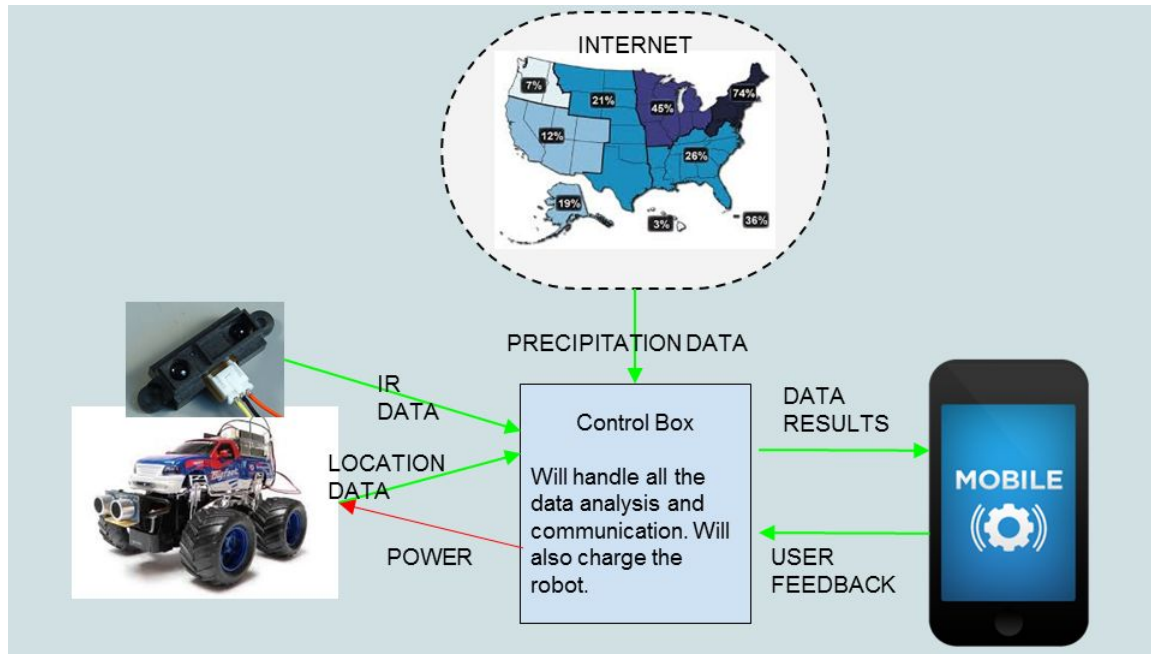
Subsystem	Subsystem Tasks	Needs
Power	Provide power to robot, charger, and controller box	Needs to be waterproof
Controller box communication	Control robot, receive and interpret information from internet	Needs to be able to remember pathing
Robot maneuvering	Allow robot to move efficiently through grassy terrain	Needs to have robot maintain composure during drilling
Robot sensing	Keep robot from hitting unexpected objects	Needs infrared technology, emergency gyroscope to detect flipping
Robot probe	Detect moisture in ground through a drill	Needs to be sturdy enough to not be damaged during drilling
Sprinkler setup	Ordinary sprinkler system, activates according to collected data	Needs to be able to branch according to what needs water
Interface app	Keeps user up to date on expected sprinkling	Needs to be simple and user-friendly
Internet connection	Connects app to weather data online, feeds info to app and controller box	Needs to have reliable connection

Daniel Miller, Tyler Castro, Michael Turner, Coy Coburn

II - Modified White paper



Subsystem	Primarily Responsible Team Member	Student Responsibilities/ Tasks
Power	Daniel	Prepare the necessary power supply for both the probe as well as the sprinkler system
Controller	Coy	Create a connection between the master controller with its slave connections; these include the probe, the sprinkler system, and the interface app
Robot maneuvering	Daniel	Enhance the robot's ability to maneuver off-terrain and possess the ability to set a route for probing locations
Robot sensoring	Michael	The robot will need the functions to sense its surroundings and take necessary precautions to avoid obstacles and safely maneuver a lawn.
Moisture measurement	Tyler	IR sensors will be set to sample water moisture in multiple locations in the lawn and reset said probe.
Mobile App	Coy	A mobile app will be created for a user to view sprinkler settings as well as make changes to planned watering for the week or its default.
Weather Data Mining	Michael	The sprinkler master controller will need to connect to weather websites via internet so to plan watering settings for the upcoming week.



POWER

Functional requirements-Provide power for the control station, provide charging capability for the robot

Design parameters- Central control must be able to provide correct power requirements for the main controller and robot charge station.

Primary constraints- Step down from 120V AC to microcontroller voltage and battery charging voltage

Limiting factors-cost, size, Portability

POWER

	Cost of power (Least important)	Size	Portability (most important)
Battery	High, frequent changing of batteries	Medium, depends on battery type	High
Wall outlet	Low	Medium	Low, needs cord
Custom (outlet/battery combination)	Medium	Medium, depends on battery type	Medium, outlet for controller but batteries for robot

POWER

We selected the combination of batteries for the robot and direct connection to a wall outlet for the station housing a charging station and the microcontroller for the entire system. The station would consume too much power to rely on batteries, and the cost would become too high. In order to keep the robot mobile, we have decided to give it batteries while allowing it to charge while not in use in the station.

CONTROLLER

Functional requirements-can send and receive data from the robot and the mobile device. Will also analyze data taken from the robot and the internet. Control the sprinklers

Design parameters-it will need reliable wifi connection with internet and robot. The system will need adequate memory to store and calculate data. GPIO pins are needed for sensor connections.

Primary constraints- TCP function is preferred, a RAM of at least 256 mB and max of 1kB flash is needed. At least 10 pins will be needed

Limiting factors-cost, processing time, memory size, Wi-Fi/bluetooth, external interfacing options, and ease of programming

CONTROLLER

	cost (most important)	processing time	memory size	Wi-Fi (least important)	external interfacing options
Raspberry Pi B+	\$29.95	700 MHz (SoC)	512 mB (RAM)	Ethernet port, can use wifi adapter	26 GPIO
RCM5400W	\$119	74 MHz (microprocessor)	512 mB (RAM)	Integrated	39 GPIO, startup, status, reset in/out
BeagleBone Black	\$55	1 GHz (SoC)	512 mB (SDRAM)	Ethernet port, can use wifi adapter	46 GPIO
TI Tiva	\$20	140 MHz	256 mB (SRAM)	Ethernet port, can use wifi adapter	40 GPIO

CONTROLLER

While most, if not all, of the choices would probably work for our controller, the TI Tiva board was chosen for its relatively cheap price and met all of the required constraints. While the Raspberry Pi B+ and Beaglebone Black were also decent choices, they are System on Chips, which is much more than we actually need.

ROBOT MANEUVERING

Functional requirements-navigate multiple terrains and location knowledge. It will also need wifi capability with the controller.

Design parameters- the motors must not deplete the battery before it has completed its circuit. Motors must also possess enough torque to move the robot.

Primary constraints- less than 10 A on battery draw, enough torque to easily move at most 2.5 kg load.

Limiting factors- torque, power usage, and cost

ROBOT MANEUVERING

	Torque (kg-cm) (40%)	Power usage (30%)	Cost (30%)
HS-422 Servo Motor	4.1	.9 (No-load) at 6.0 V	\$9.69 * 2
DC Toy / Hobby Motor	.02	.42 W (No-load) 1.5 W (loaded) at 6.0 V	\$1.95 * 2
2WD microcontroller platform	1.92	.426 W (No load) 2.82 W (loaded) at 6.0 V	\$22.49
B0081C5B80	.08	1.5 W (loaded) at 6.0 V	\$6.40 * 2

ROBOT MANEUVERING

The 2WD microcontroller platform has a relatively nice balance of torque and power consumption, but is the highest in cost. The HS-422 Servo Motor has the highest power consumption, but the highest torque. High torque is necessary for allowing our robot to traverse through grass easier, so the HS-422 Servo Motor is the motor we have decided on.

ROBOT SENSORS

Functional requirements- object avoidance, Bluetooth capability with the controller box.

Design parameters- Distance at which installed sensor discovers an obstruction, time taken to correct pathing

Primary constraints- Correction time must be quick enough to keep from colliding with obstruction, to preferably keep the robot continuously running

Limiting factors- cost, sensor accuracy, reaction time, and distance

ROBOT SENSORS

	Cost (60%)	Distance (40%)	Overall (of 10)
PING))) Ultrasonic Distance Sensor	5	2	3.8
PmodMAXSONAR - Ultrasonic Range Finder	4	10	6.4
Devantech SRF05 Ultrasonic Range Finder	6	2	4.4
Sharp GP2Y0A21YK0F Analog Distance Sensor 10-80cm	8	6	7.2

ROBOT SENSORS

Although the PmodMAXSONAR - Ultrasonic Range Finder is very effective and has a massive range, the tradeoff for its cost of \$30 doesn't stand up to the overall quality of the [Sharp GP2Y0A21YK0F Analog Distance Sensor 10-80cm](#). The range of the PmodMAXSONAR is unnecessary, with it's maximum range of 645 cm, and the range of the Sharp Sensor is satisfactory while at a third of the price.

MOISTURE MEASUREMENT

Functional requirements-moisture detection, data transmission

Design parameters- Current readings from the two photodetectors, voltage difference of the two voltages after passing through the transimpedance amplifier, output of the comparator

Primary constraints- For the diodes, forward voltage must not exceed 1.55 V, and reverse voltage must not exceed 5 V.

Limiting factors- accuracy, cost, quality

MOISTURE MEASUREMENT

	Accuracy (50%)	Cost (50%)	Overall (of 10)
THORLABS LED910E NIR LED	5	9	7.5
THORLABS LED1050E NIR LED	7	5	6
THORLABS LED1550E NIR LED	8	3	5.5
THORLABS FGA01 Photodetector	8	1	4.5
DigiKey 751-1006-ND Photodetector	5	10	7.5

MOISTURE MEASUREMENT

In order to get the highest amount of accuracy from the photodetector/NIR LED combination, we would want the highest difference in wavelength between the two LEDs, as that would create the largest difference in absorption from water, allowing for greater precision in voltage difference. However, price becomes an issue when purchasing higher wavelength LEDs. Although the price of the 1050 and 1550 nanometer LEDs is the same from THORLABS, the price of a photodetector in the spectral range for 1550 nanometers skyrockets to ~\$50 for the THORLABS FGA01, compared to DigiKey's 751-1006-ND, which is priced at around \$1. Therefore, the sufficient tradeoff would be to use the 910 and 1050 nanometer LEDs paired with two 751-1006-ND photodetectors, which both fall within the spectral range, while keeping price to a minimum.

MOBILE APP

Functional requirements-real-time notification of sprinkler settings to user, user ability to modify sprinkler settings.

Design parameters-an eye-pleasing GUI is preferred for use, simple buttons and toggles for user interaction is required.

Primary constraints- operate available memory given through mobile app

Limiting factors- GUI, ease of use, and development time

MOBILE APP

	GUI (least important)	Ease of use (most important)	Development time
Android	Free GUI Android set	Open-source	Simple
IOS	iPhone GUI PSD	Closed-source	Complex
Windows	NET/XAML, Win32	Closed-source (technically)	Medium

MOBILE APP

The team has chosen to use Android app development system. While not only is Android an open-source model, recent news has shown that Android apps will also be usable on Windows phones, increasing the amount of potential users. It is also a pro that Android development is a common beginning for many application programmers. This can be seen with the amount of help and tutorials on designing mobile Android app interfaces and functions.

WEATHER MINING DATA

Functional requirements- ability to connect to interweb and retrieve weather data

Design parameters- choosing language that allows for most firmware/internet interaction via sockets, and the choice of weather websites

Primary constraints- accuracy of website, versatility

Limiting factors- runtime, complexity, and design

WEATHER MINING DATA

	Runtime (Most Important)	Complexity (Least Important)	Design
Java	High	Higher-level	Application oriented
C++	Low	Low-level	Hardware oriented
Python	Medium	Low-level	Web oriented

WEATHER MINING DATA

We have chosen to build our program on C++ for its hardware oriented design, which will prove useful when interfacing with the board. While not as easy to manipulate the internet compared to web-oriented Python, it still has complete functionality with usage of sockets.

Team 24 Ground Penetrating Radar

Subsystem	Subsystem Tasks	Subsystem Specs
Power	Provide power to the robot and controller	Step down from 120V AC to voltage requirements for robot and controller.
Controller	Receive and interpret data sent by the robot	A reliable wifi connection is needed, and TCP packaging is preferred for data transfer.
Controller	Receive and interpret information from internet	A reliable wifi connection is needed, and TCP packaging is preferred for data transfer.
Controller	Calculations made to create sprinkler settings for upcoming week	256 Mb to calculate sprinkler settings from received data, and 1 Mb flash to store settings made from calculations.
Robot maneuvering	Allow robot to move efficiently through grassy terrain	Motors need enough torque move and turn robot at least 2.5 kg. Also possibly 4 motor-powered wheels for slopes and muddy terrain.

Subsystem	Subsystem Tasks	Subsystem Specs
Robot sensors	Measure distance of foreign objects in front of robot	Measurable distance of at least 50 cm in front of robot to allow for turning.
Moisture measurement	Detect moisture in lawn section	Voltage in diode circuit must not exceed its listed voltage maximums in datasheets.
Moisture measurement	Send found data to controller	A reliable wifi connection is needed, and TCP packaging is preferred for data transfer.
Interface app	Keeps user up to date on expected sprinkling	Needs to be simple and user-friendly, sends at least 3 notifications a week
Interface app	Give user ability to influence sprinkler settings	App should have tabs/toggles for time/day of watering, time amount for watering, sections to water, and setting to turn on/off sprinkler system.
Weather Mining Data	Connects app to weather data online, feeds info to app and controller box	Needs to have reliable connection

Daniel Miller, Tyler Castro, Michael Turner, Coy Coburn

III - Project Change

During the middle of November, the team switched from the Smart Sprinkler Project to the Ground Penetrating Radar. This was presented to us by the TA at the time, Chadi Geha. Immediately the team focused on planning and researching our new project. The team used the time during the weekly meetings to go over research made, specifications that relate to RF architecture design, and how to implement certain techniques to meet the requirements set by the sponsor Dr. Everett.

IV - Proposal

GPR Root Mapping System

Pre-Proposal
12/14/15

ECEN 403 – Capstone (Senior) Design
Texas A&M University, College Station, TX

Team24
Tyler Castro
Coy Coburn
Daniel Miller
Michael Turner

Daniel Miller, Tyler Castro, Michael Turner, Coy Coburn

Abstract

The goal of this project is to create a ground penetrating radar system to serve as a non-destructive method for mapping plant root systems. The system consists of two antennas, one for receiving and one for transmitting, a control unit and power supply.

A control unit will be used to pass an electrical pulse to an antenna. The antenna will transmit the signal into the ground at a frequency of 915 MHz. The signal will reflect off materials with different dielectric constants like that of roots and pipes. The strength and time required for the return of any reflected signal is measured and recorded.

Once the signal is received, the scanner will record and process the radio signals into digital signals and process an image of the recorded data for display to the user. This data is collected over a given area and a computer, using specialized software, will apply mathematical functions to the signal in order to remove background interferences. Over multiple instances, the user will have enough data from the images to observe the change in the soil composition due to the actions of the root systems absorbing and transferring water and nutrients from the soil. The software will display the strength of the reflected signal with respect to time and position in a 2-D image.

Power being delivered to the antennas must be regulated to allow the generating antenna to propagate radio waves with high enough energy to overcome the attenuation that happens as the wave travels through the ground. Output power is to be regulated according to the type of soil being penetrated, as well as the plant type to be mapped.

I. INTRODUCTION

A. Need Statement

Root growth is complex and little is known about the reason behind root development patterns. Better understanding roots will offer deeper insight into water and nutrient flow in an ecosystem, but observing root growth in an ecosystem over a period of time can be difficult, and no good non-destructive methods are in place. A ground penetrating radar system allows for the observation of root growth while preserving the wellbeing of the ecosystem. . Research utilizing this project's device can lead to improvement in farming techniques, minimizing damage to the environment from human interaction, aid in hydrogeophysics contributions, as well as quicker soil replenishment and reforestation.

B. Proposed System

The ground penetrating radar system can be broken down into four subsystems as shown in Figure 1: Power, Control Unit, Antennas, and Signal processing/Display.

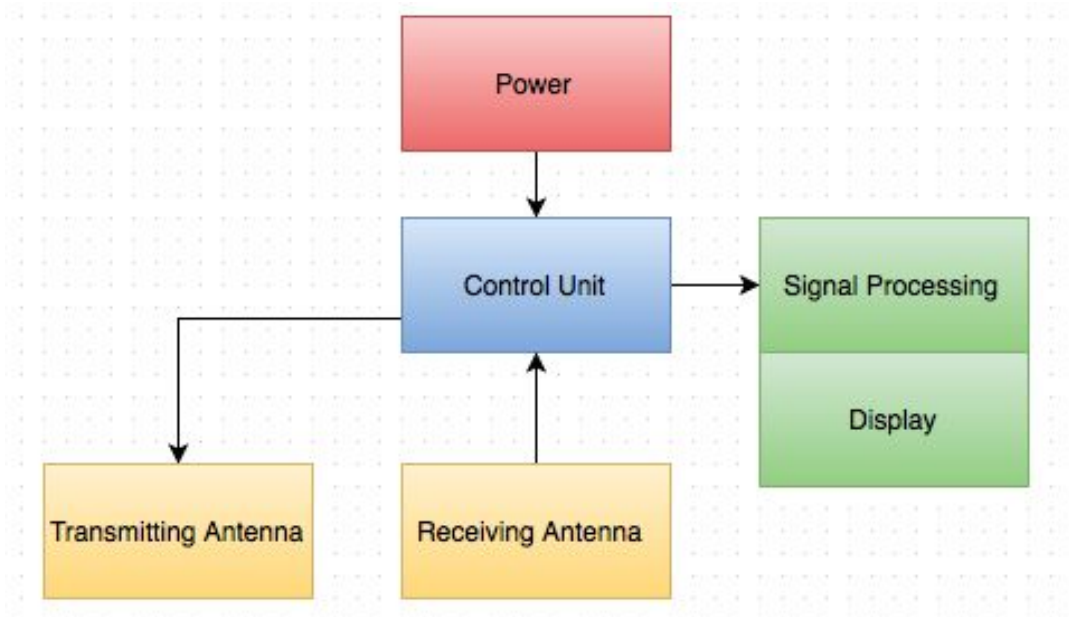


Fig. 1. System
block diagram

The ground penetrating radar system depicted in Figure 2 works by using antennas to send an electrical pulse into the ground and record the strength and the time required for the return of any reflected signal. This technique uses high-frequency pulsed EM pulses (from 10 to 3000 MHz) sent into the ground to discover what is underneath. Reflections are produced when radio waves pass through materials with different electrical conductivity; some of the original signal is reflected while some continues to travel in the material until it reaches another boundary where more of the signal is reflected or until the signal dissipates. These reflected signals are collected using another antenna and passed into a digital processor that will create a 2-D image using mathematical

functions.

Contrary to most ground penetrating systems, we chose to use phased array antennas at a frequency of 915MHz. A phased array antenna is exactly what it sounds like, an array of antennas spaced half a wavelength apart. If the antenna is designed correctly, by passing the signal through all antennas at the same time, the sinusoidal waves produced will constructively and destructively interact with each other so that a single wave will travel in the desired direction and cancel each other out in all other undesired directions. This will help to reduce noise in the receiving antenna.

This frequency was selected because of the high resolution needed to detect plant roots. Low frequencies (1-500MHz) are used in ground penetrating radar systems where a large depth of penetration is required. Higher frequencies have lower penetration depths because more of the signal is reflected off boundaries between different dielectric properties like that of roots. We chose this frequency because of its depth of .7 meters, which is the optimum depth to observe root growth.

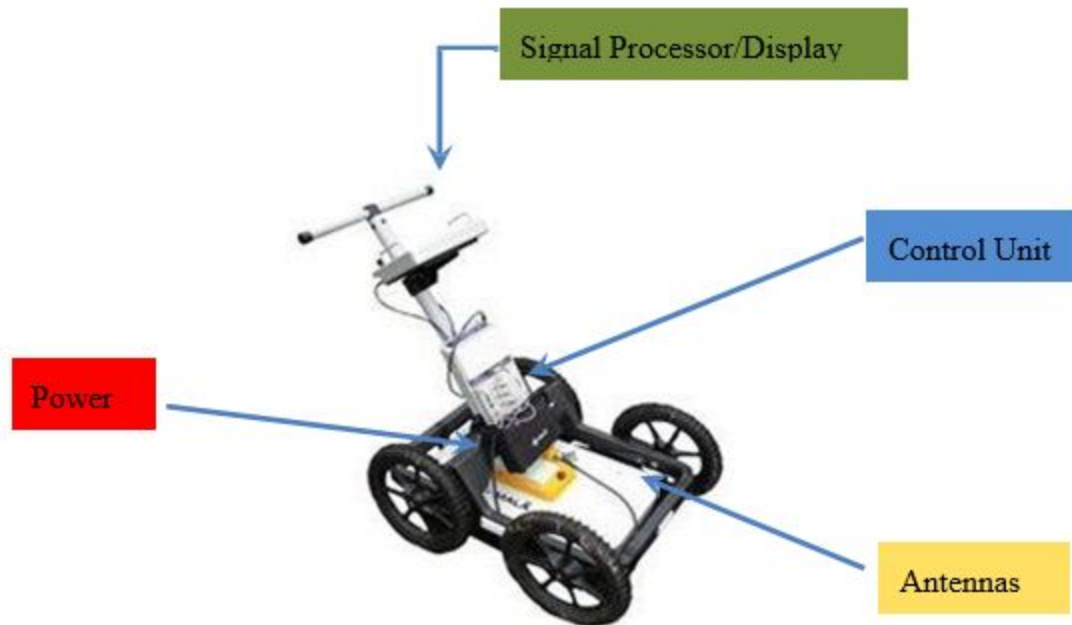


Fig. 2. Physical Sketch of
the System

Material	Relative Permittivity, K	Pulse Velocities, m/Ns	Conductivity, mS/m
Sand (dry)	4-6	0.15-0.12	0.0001 - 1
Sand (saturated)	25	0.055	0.1 - 1

Table 1: Surface material and notable attributes

The propagation of the transmitted signal depends on electrical properties of the materials that the signal is reflected off. The dielectric constants of these materials will influence the signal's echo and will be revealed in the data collected by the

receiver. GPR can be done either by continuous profiling or stationary point collection. While continuous may be quicker to cover more area, the data received is not nearly as detailed or accurate. For the project's scope, stationary point collection will be the better choice given its method to stack scans multiple times for more accurate results before moving to the next area to be scanned.

Relative Permittivity	1	5	10	15	25	80
Frequencies						
100 MHz	3	1.36	0.96	0.76	0.6	0.32
200 MHz	1.52	0.68	0.48	0.4	0.32	0.16
300 MHz	1	0.44	0.32	0.24	0.2	0.12
500 MHz	0.6	0.28	0.2	0.16	0.12	0.08
900 MHz	0.32	0.16	0.12	0.08	0.08	0.04

Table 2: Radar Wavelengths for Antenna Frequencies and Relative Permittivity

II. CONCEPTUAL DESIGN DESCRIPTION

A. Implementation Transmitting Antenna

The design of the transmitting antenna is shown below in Figure 3. The coaxial oscillator will be connected to a switch, which will be controlled by the microcontroller. The microcontroller can be programmed to control the pulse repetition frequency and pulse duration by completing the circuit for a period of time. A pulse from the oscillator will pass through an attenuator and a power amplifier before being sent through the antenna array. The attenuator helps with impedance matching with the antenna, and will lower the Voltage Standing Wave Ratio in order to have minimal power reflection when fed to the antenna. The low noise power amplifier will increase the power of the pulse passed through it, which will give the pulse a large signal-to-noise ratio, allowing for clearer images to be created after signal processing. Before reaching the antenna, the pulse will also go through a power splitter. The splitter will branch the pulse with minimal insertion loss, so the pulse can then also be sent to the receiving end of the antenna system for signal mixing.

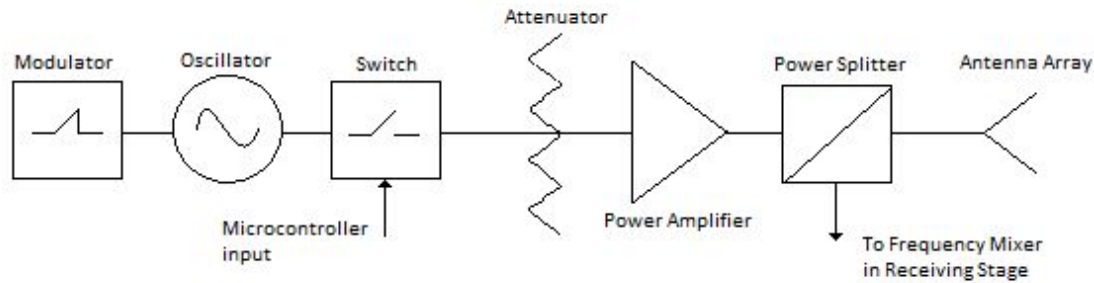


Figure 3: Transmitting Antenna design

The modulator shown in figure 3 is used to implement frequency modulation for pulse compression, as explained in the following section.

Pulse Compression

Pulse compression will also be implemented in our system design, which will increase range resolution and signal to noise ratio, and allow us to balance pulse duration and consumed power. Pulse compression can be achieved through either frequency modulation, or phase modulation [1].

For frequency modulation, our input pulses can be modified to have a frequency that changes linearly over the period of the pulse. This type of signal is referred to as a linear chirp. When the received chirp is inter-correlated with our original chirp, the resulting signal has a smaller width than the original. This improves our resolution, because received signals that are shorter in time mean that reflections can be closer together without blending together. A visual example of frequency modulated pulse compression is shown in figure 4. In order to change our input pulses to chirps, a modulator can be inserted, which will produce a linear ramp function. This ramp function will be fed into the Vtune input pin of the oscillator, which will cause the input voltage to be proportional to the transmit frequency, creating linear chirps.

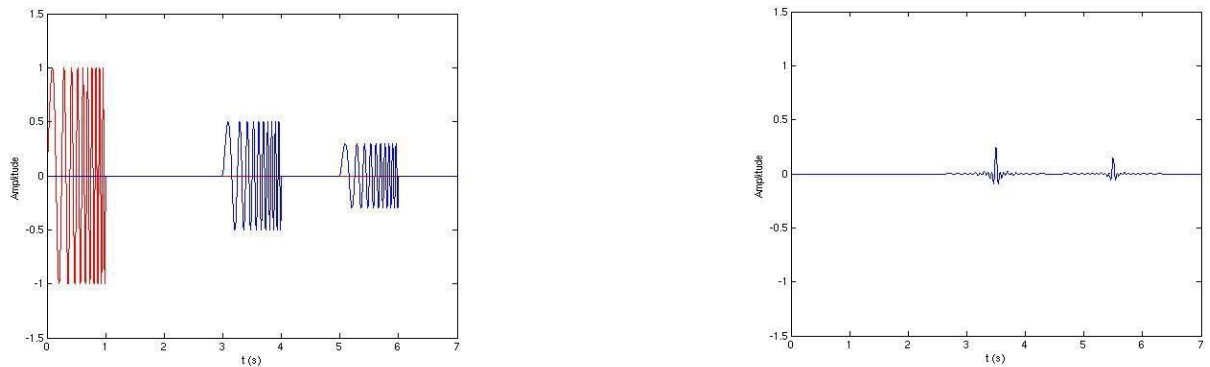


Figure 4: Linear chirp with two reflections, and the resulting echoes from matched filtering [2]

For phase modulation, the input pulse can be modified to be broken up into a series of time slots with equal duration. These slots can be assigned a phase of either 0 or 180 degrees. There are sequences of phases that, when correlated with itself, create a resulting pulse with large side lobe level ratios. For example, taking the original pulse and splitting it into two, with the first half of the pulse having a phase of 180 degrees and the second half having a phase of 0 degrees, relates to the Barker code of +1, -1. Correlating that pulse with itself creates a pulse with side lobe level ratios of -6 dB. To create this example in our circuit, another switch could be inserted to direct the first half of the pulse through a phase shifter of 180 degrees, then switch to another line without the phase shifter for the second half of the pulse. However, this will be difficult to achieve, as the speed of the switch would have to be impossibly fast.

Phased Antenna Array

With an antenna array, phase shift modules can be used to alter the phase of individual antennas and direct the total radiation pattern and direction of the system. For the proposed system, the array's total radiation pattern can be directed to focus on a specific point to increase the total energy of radiation. This would be helpful for when the ground has high water concentration and attenuates RF waves greatly.

A passive phased array, where there is a single source of RF waves and a phase shift module for each antenna in the array, would be the easiest implementation. A block diagram of a passive phased array is shown in figure 6. Due to destructive and constructive interference, an array of antennas has a high gain width, and low sidelobes, with the gain centered in the middle of the array. The direction of the main lobe can be altered using the phase shifters.

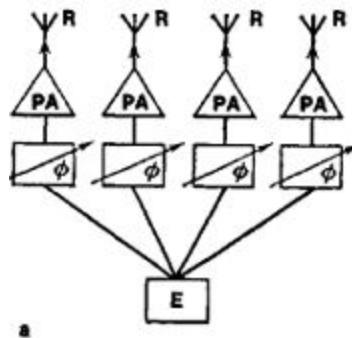


Figure 6: A general representation of a passive 4 antenna phase array [3]

Antenna Choice

Because we only need the pulse directed in a specific area, directional antennas were looked into for use in this project, as opposed to omnidirectional antennas. After researching previously used antennas in similar projects, the horn antenna seemed to be the most used type of antenna for GPR. Because horn antennas have no resonant elements, they have a wide bandwidth, and have high antenna gain [4]. However, they are not easily constructed, and are more expensive than antennas of more simple design. The Vivaldi antenna co-planar directional antenna with a wide bandwidth. Vivaldi antennas are of simple design, making them low-cost. Their combination of efficiency in both performance and price makes Vivaldi antennas the choice for this project. A simple diagram of a Vivaldi antenna is shown in figure 7.

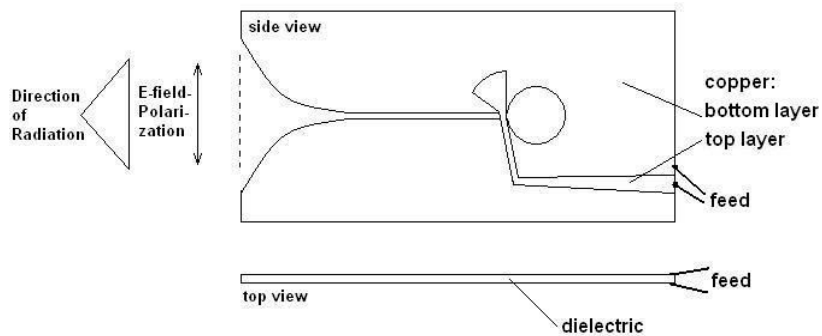


Figure 7: A Vivaldi Antenna

Receiving Antenna

The receiver will convert the received echo signals into a digital signal to obtain the reflected information. The receiver will need to be sensitive, have a large fractional bandwidth, good noise performance, and a large dynamic range. The receiver hardware will include a time varying gain (TVG), a low noise amplifier (LNA), and sample and hold (S/H) circuit unit.

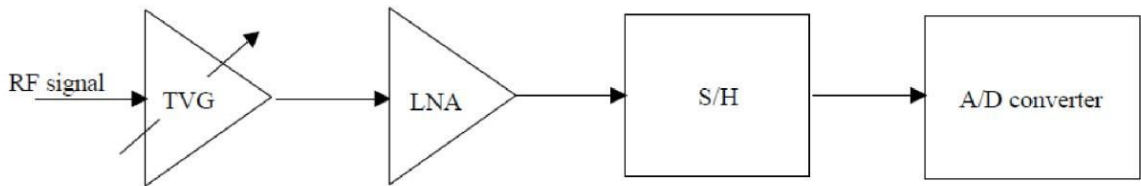


Figure 8: Block Diagram of Receiver Antenna []

The TVG's purpose is to compensate for spreading losses of the transmitting signal and reflected echo. This is done by introducing a fixed gain in dB per unit in time (or distance). In reality, the TVG is an attenuator based in PIN diodes that can have a variable resistance as a function of voltage. Since the first and largest reflectance is the air-ground interface, the reflections in the ground will be seen later in time and are less attenuated. This allows for the LNA following the TVG to be more sensitive and therefore increasing the range of the receiver.

The LNA conditions the entering RF signal to utilize the whole dynamic range.

This is a necessity due to losses mentioned earlier in the TVG section and to ensure that most, if not all, objects in the ground are noticed and recorded in the reflected signals.

The S/H circuit unit provides a constant stable signal value for the A/D converter. The input bandwidth must be of the same order as the highest frequency received. A full-bridge sampler circuit has been chosen for its good linearity, noise performance, and common usage with frequencies under 1 GHz.

With A/D converters that have conversion rates of 200 MHz for 8 bit and 10 MHz for 16 conversions, a technique is to slow down the sampling rate. Sequential sampling can do this by converting on intersections of the slow and fast ramps, which are determined by the wanted number of samples and PRF rate. Conversions done by the actual A/D converter with 16 bits can have a dynamic range of 96 dB.

B. Analysis

Penetration depth

Penetration depth of microwave and RF power is defined as the depth where the power is reduced to 1/e or 36.7% ($e=2.718$) of the power entering the surface [5]. The penetration depth of a signal as a function of frequency is shown below (1). Using a frequency of 915 MHz and a complex relative permittivity of sand at 20% moisture content with $\epsilon^*= 20.3 - j1.17$ [1], the penetration depth was calculated to be .201 meters. Another calculation of penetration depth was done for sand with a moisture content of 4% which resulted in a penetration depth of .733 meters. This shows that moisture content is a large factor in calculating penetration depths and determining the moisture content of the soil before scanning is important. Note: this calculation only shows penetration depths meaning once the signal reflects off an object the signal will then experience an equivalent loss traveling back to the receiving antenna. For this reason, a high power signal must be sent so that the signal can travel to these depths and return with enough power for the antenna to receive.

$$dp = \frac{c}{2\pi f \sqrt{2\varepsilon'(\sqrt{1+(\frac{\varepsilon''}{\varepsilon'})^2}-1)}} \quad (1)$$

$$.201 \cong \frac{3E8}{2\pi(915E6) \sqrt{2(20.3)(\sqrt{1+(\frac{1.17}{20.3})^2}-1)}} \quad (20\% \text{ MC}) \quad (1)$$

$$.733 \cong \frac{3E8}{2\pi(915E6) \sqrt{2(3.33)(\sqrt{1+(\frac{.13}{3.33})^2}-1)}} \quad (4\% \text{ MC}) \quad (1)$$

References

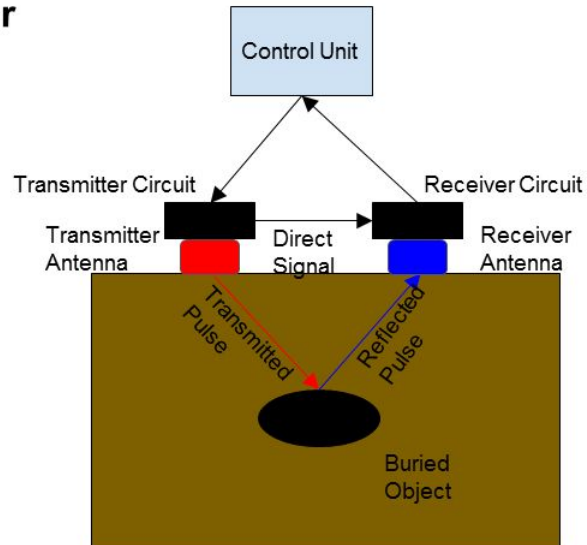
- [1] C. Allen , “Radar Pulse Compression ,” 2004. [Online]. Available at: https://www.ittc.ku.edu/workshops/Summer2004Lectures/Radar_Pulse_Compression.pdf. [Accessed: 2015]
- [2] Flambe , "Chirp before" and "Chirp compr" 2006. [Online]. Available at: https://commons.wikimedia.org/wiki/File:Chirp_before.jpg#/media/File:Chirp_before.jpg and https://commons.wikimedia.org/wiki/File:Chirp_compr.jpg#/media/File:Chirp_compr.jpg. [Accessed: 2015]
- [3] “Phased Array” 2003. [Online.] Available at: <http://encyclopedia2.thefreedictionary.com/Phased+array+radar>. [Accessed: 2015].
- [4] “The Horn Antenna” 2009. [Online.] Available at: <http://www.antenna-theory.com/antennas/aperture/horn.php>. [Accessed: 2015].
- [5] V. Komarov, S. Wang, and J. Tang , “Permittivity and Measurements ,” 2005. [Online]. Available at: <http://public.wsu.edu/~sjwang/dp-rf-mw.pdf>. [Accessed: 2015].
- [6] Cedric Martel, “Modelling and Design of Antennas for Ground-Penetrating Radar Systems ,” Ph.D. dissertation, Dept. Elect. Eng, Univ. of Surrey, Guildford, United Kingdom, 2002.
- [7] “Ground Penetrating RADAR (GPR) (After Basson 2000) Introduction,” GPR theory, 2007. [Online]. Available at: <http://www.geo-sense.com/gprmore.htm>. [Accessed: Jan-2015].
- [8] Standard Guide for Using the Surface Ground Penetrating Radar Method for Subsurface Investigation, Active Standard ASTM D6432, 2011
- [9] A. P. Annan, "Ground Penetrating Radar Principles, Procedures & Applications," Sensors & software Inc., Mississauga, Ontario, 2003
- [10] Bart Scheers, “Ultra-Wideband Ground Penetrating Radar, with Application to the Detection of Anti Personnel Landmines,” Ph.D. dissertation, Dept. Elect. Eng, Catholic Univ. of Louvain, Louvain-la-Neuve, Belgium, 2001.

V - CDR Presentation

Ground Penetrating Radar

Team 24
 Tyler Castro
 Coy Coburn
 Daniel Miller
 Michael Turner

- Objective:** To map underground root systems
- The transmitter will pulse a signal to penetrate the ground.
- The receiver will take the reflected signal.
- The control unit will display the created radar image and record an image log.
- The main feature of this GPR system is the phased array antennas.**



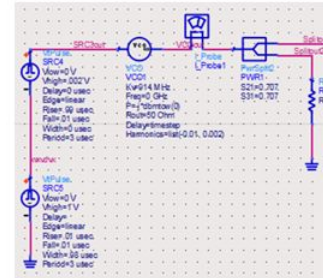
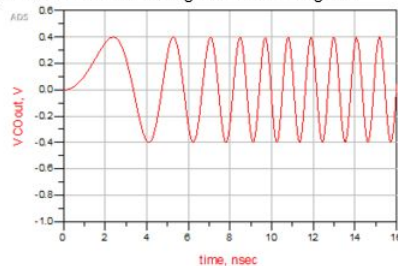
Subsystem	Primarily Responsible Team Member	Student Responsibilities/ Tasks
Transmitter Circuit	Tyler	Design and implement the circuit to transmit the RF signal as well as utilize pulse compression via chirping the signal.
Transmitter Antenna	Daniel	Design phased array antenna for generating signal
Receiver Antenna	Coy	Successfully catch reflected signals and mix said signals for A/D conversion.
Receiver Circuit	Michael	Design the receiver components and verify that they adjust the signal properly before mixing.
Control Unit	Coy	Allow for user manipulation of the GPR device and image processing for the radar display.

Tyler Castro

A modulator generating a sawtooth signal is connected to a voltage controlled oscillator

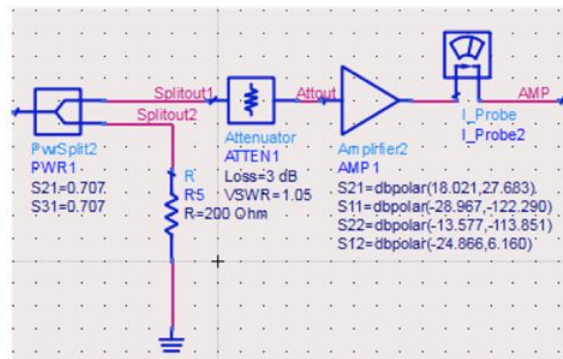
Resulting signal is a linearly modulated chirp, with frequency from 902 to 930 MHz

A chirp allows for better filtering on the receiving end



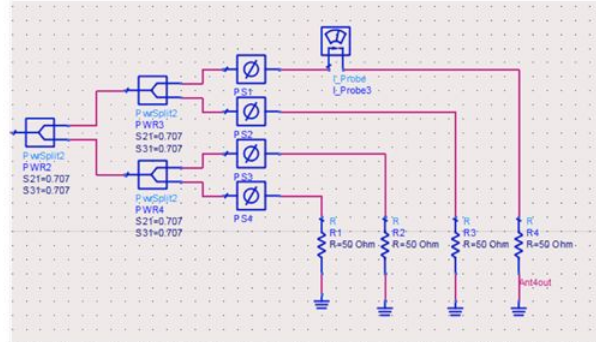
Daniel Miller

- Splitter for sending to a mixer on the receiving end
- Attenuator for impedance matching
- Amplifier S-parameters based off of an PA of 11 dB gain, ZX60-3011+

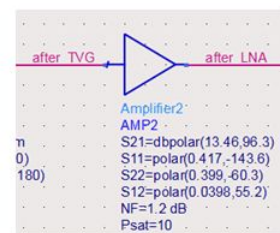
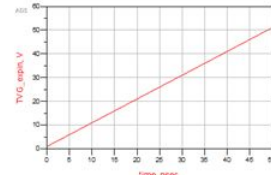
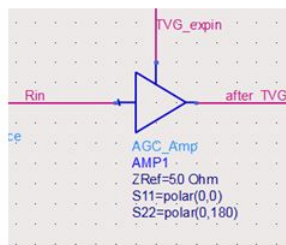
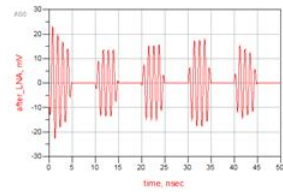
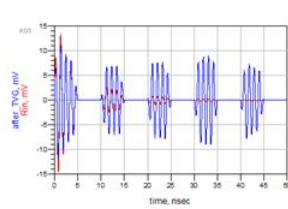
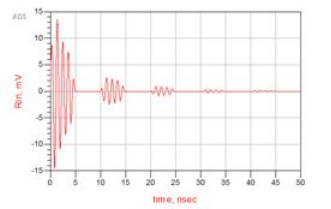


Daniel Miller

- 50 ohm resistors used to represent antenna load
 - Phase shifters used to direct or focus antenna pattern



Michael Turner



Semester 2

Period Highlight: 1 Plan Actual % Complete

ACTIVITY	PLAN	PLAN	ACTUAL	ACTUAL	PERCENT	PERIODS
	START	DURATION	START	DURATION	COMPLETE	
Finalize ADS	1	2	1	2	90%	1
Research Hardware	1	2	1	2	50%	2
Buy Hardware	2	4	2	4	0%	3
Build test area	4	1	4	1	0%	4
Install	3	7	3	7	0%	5
Control Unit	5	6	5	6	0%	6
Progress Report	7	2	7	2	0%	7
Test Transmitter(Output)	7	5	7	5	0%	8
Test Receiver	7	5	7	5	0%	9
Finalize	10	3	10	3	0%	10
Final Project Presentation	13	3	13	3	0%	11
						12 13 14 15 16 17 18 19 20

Summary/Conclusion

In summary, both the transmitter and receiver subsystems are the main focus for the team as a whole at the moment. Once simulations have been finalized, hardware will be bought and installed which will occupy most of the semester. The control unit subsystem will then be the main priority along with field testing of the GPR. While there is much work that still needs to be done, progress so far is encouraging.

VI - Mid Term Report

Ground Penetrating Radar

Team 24 Progress Report

March 6 2016
ECEN 404 – Senior Design Project
Texas A&M University, College Station, TX

Daniel Miller
Michael Turner
Tyler Castro
Coy Coburn

Abstract

The goal of this project is to create a ground penetrating radar system to serve as a non-destructive method for mapping plant root systems. The system consists of a transmitting and receiving antenna and circuitry for both the transmitter and receiver. The transmitting circuit generates a linear frequency-modulated continuous wave from 2.4- 2.475GHz. The wave is pulsed to avoid interference between the transmitting and receiving antenna. The transmitting antenna passes the generated signal into the ground while the receiving antenna collects the reflected signal. The signal will reflect off materials with different dielectric constants like that of roots and pipes. The received signal will then be sent through an LNA for amplification to balance any loss of gain. The signal is also fed into a frequency mixer to correct any occurred frequency shift. Finally, the IF signal is converted into digital data that will be recorded for image processing.

Table of Contents

Abstract

Table of Contents

1 Project Overview

- 1.1 Proposed System
- 1.2 Project Deliverables
 - 1.2.1 Project Specifications
 - 1.2.2 Significant Direction Changes
- 1.3 Project Timeline and Task Ownership

2 Subsystem Antennas

- 2.1 Significant Changes in Direction
- 2.2 Subsystem Specifications
- 2.3 Subsystem Status
- 2.4 Subsystem Technical Details
- 2.5 Subsystem Testing
 - 2.5.1 Validation of Antenna Specifications

3 Subsystem Receiver Circuit

- 3.1 Significant Changes in Direction
- 3.2 Subsystem Specifications
- 3.3 Subsystem Status
- 3.4 Subsystem Technical Details
- 3.5 Subsystem Testing
 - 3.5.1 Schottky Diode
 - 3.5.2 PIN Diode Driver

4 Subsystem Signal Generation

- 4.1 Significant Changes in Direction
- 4.2 Subsystem Specifications
- 4.3 Subsystem Status
- 4.4 Subsystem Technical Details
- 4.5 Subsystem Testing
 - 4.5.1 VCO output

5 Subsystem Receiver Signal Converter

- 5.1 Significant Changes in Direction
- 5.2 Subsystem Specifications
- 5.3 Subsystem Status
- 5.4 Subsystem Technical Details
- 5.5 Subsystem Testing
 - 5.5.1 Mixer induced frequency shift

Daniel Miller, Tyler Castro, Michael Turner, Coy Coburn

[6 Conclusions](#)

[References](#)

[Appendix A Project Budget](#)

[Appendix B Subsystem Schematic](#)

[Function Generator Schematic](#)

[Receiver Circuit Diagram](#)

List of Figures

[Figure 1.1: System block diagram.](#)

[Figure 1.2: Gantt Chart](#)

[Figure 2.1: Figure 2.1: Vivaldi Antenna Diagram, with microstrip feedline](#)

[Figure 3.1: Schottky test circuit diagram](#)

[Figure 3.2: PIN diode driver test circuit diagram](#)

[Figure 5.1. Typical output phase noise plot for the AD9834](#)

List of Tables

[Table 1.1 Specification Compliance Matrix](#)

[Table 1.2 Responsibility Matrix](#)

[Table 2.1 Antenna specification Compliance Matrix](#)

[Table 2.2 Antenna Design](#)

[Table 3.1 Receiver Circuit specification Compliance Matrix](#)

[Table 4.1 Signal Generation specification Compliance Matrix](#)

[Table 5.1 Signal Generation specification Compliance Matrix](#)

[Table A-1 Project Budget](#)

[Table B-1 BOM for Signal Generation](#)

[Table B-2 BOM for Receiver Circuit](#)

1 Project Overview

The GPR root mapping systems will locate plant roots underground using radar waves emitted and received by arrays of antennas. Mathematical equations will be applied to the reflected signal so the user can interpret the data. Geophysicists can use this data to examine plant root growth over a period of time.

1.1 Proposed System

The transmitting circuit will generate a continuous wave RF signal with a linearly swept frequency from 2.4025 to 2.4775 GHz. This signal will be fed into the transmitting antenna, which will propagate the wave into the ground. Waves that are reflected off of objects underground will be picked up by the receiver antenna and run into the receiver circuit. The receiver circuit will amplify the signal before passing it to the demodulator, which will convert it to digital point for future signal processing.

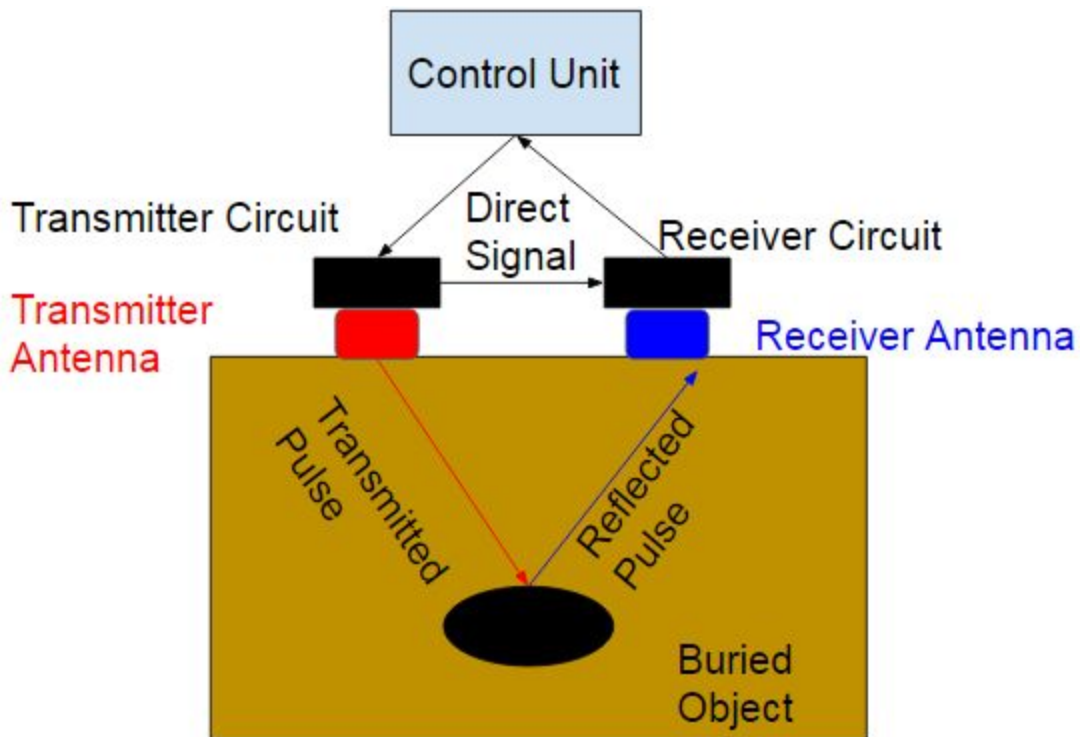


Figure 1.1: System block diagram.

1.2 Project Deliverables

By the end of the semester, we plan to have a working radar system that is able to detect roots 2 inches wide and 4 feet deep in sand.

1.2.1 Project Specifications

The transmitted signal will reach a ground depth of at least 0.7 m and up to 1.2 m. The spatial resolution will be at most 7.62 cm (3 in). There will be at least one working channel from transmitter to receiver

Daniel Miller, Tyler Castro, Michael Turner, Coy Coburn

circuitry through vivaldi antennas. These two vivaldi antennas will be specifically designed to transmit through sand with a dielectric constant of 6 at a frequency from 2.4 - 2.475 GHz. Once the received signal has been converted into digital form, the data will be recorded and stored into files that can be sent to systems for image processing.

Table 1.1
Specification Compliance Matrix

Specification	Min	Nominal	Max
			1
Ground Depth	.7 m	-	1.2 m
Spatial Resolution	-	-	7.62 cm
Operation Frequency	2.4 GHz	-	2.75 GHz

1.2.2 Significant Direction Changes

The project has recently been altered to operate using a single channel, or only one transmitting and one receiving antenna. Once a single channel has been implemented, we then look towards implementing an array of antennas. This is due to time constraints, and the importance of pure functionality over the less important array feature. Additionally, the frequency range has been heightened considerably, from a center frequency of 915 MHz to a center frequency of 2.44 GHz. This helps our resolution greatly, but hinders our penetration depth into the ground. The penetration depth is to be improved by providing more power to our signals. The change in frequency is also due to our shift away from pulse compression to continuous wave, which will lower the complexity and cost of our system by eliminating the use of SAW filters.

1.3 Project Timeline and Task Ownership

Tyler Castro is responsible for the design and construction of antennas that are able to operate properly in the frequency range required of the system. He will also test the antennas using a network analyzer to determine optimal specifications. Daniel Miller is responsible for signal generation. He calculated the power loss through the media and estimated the amount of power needed at the output of the antenna as well as throughout the transmitting circuit. Michael Turner is responsible for the design and construction of the receiver circuit. The receiver circuit must be able to amplify the signal obtained from the receiver antenna and pass it to the receiver signal converter. Coy Coburn is responsible for the design and construction of the receiver circuit that will mix, demodulate, and convert the received analog signal into digital data.

Table 1.2
Responsibility Matrix

Subsystem	Responsible Engineer	Responsibilities
Antennas	Tyler Castro	Design and build antennas, and optimize performance
Signal Generation	Daniel Miller	Design and build the transmitter circuit for the generated signal.

Team 24 Ground Penetrating Radar

Receiver signal converter	Coy Coburn	Design and build the receiver circuit that will mix and demodulate the incoming signal.
Receiving Circuit	Michael Turner	Design and build the receiver circuit that will amplify the incoming signal

Below is the Gantt Chart for the 404 semester.

Daniel Miller, Tyler Castro, Michael Turner, Coy Coburn

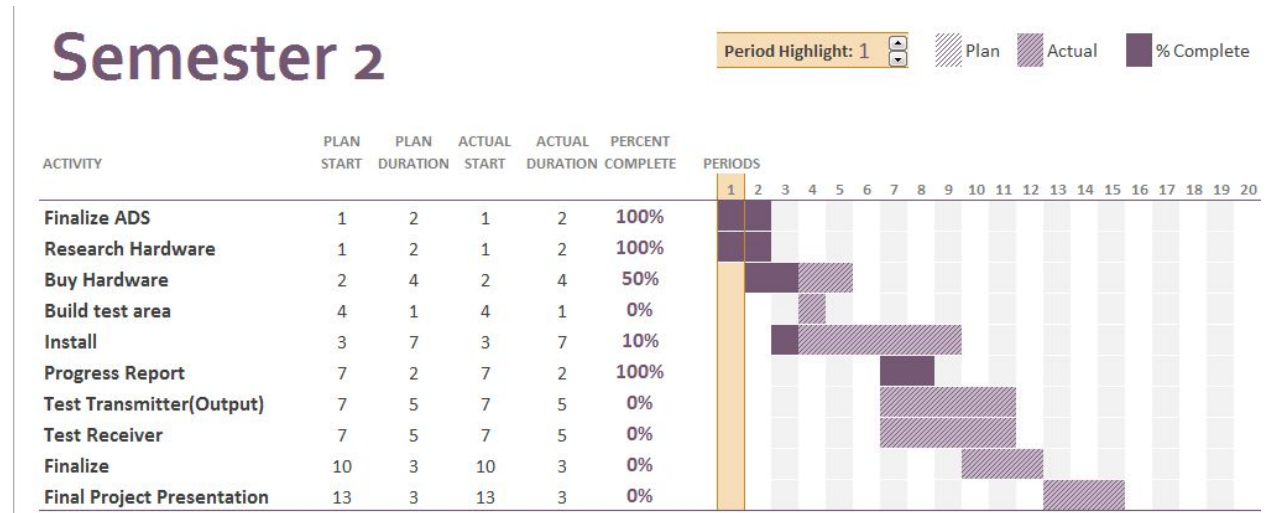


Figure 1.2: Gantt Chart

2 Subsystem Antennas

The antennas are responsible for both propagating the signal generated by the transmitting subsystem into the ground, as well as receiving the reflections of the signals that reflect off of objects in the ground. The initial design will have a single transmitting and a single receiving antenna. An array of antennas will be implemented once a single channel is proven to be working. An input signal will be fed into a balun that will prevent current from flowing along the outside of the unbalanced coaxial cable once it reaches the balanced antenna. The output of the balun will be soldered to the sides of a vivaldi antenna, cut from sheet metal and placed in a plastic tube with measurements calculated for a frequency propagation between 2.4 - 2.5 GHz, which will be pointed to the ground. Reflections from objects buried underground will be picked up by another antenna, also connected to a coaxial cable that will serve as the input to the receiving subsystem.

2.1 Significant Changes in Direction

The Antenna Subsystem was created rather recently, as joint efforts were previously being made to create a working transmitting system. The main change in direction is that the antenna is no longer planning to be mounted to a substrate, but rather be suspended in a medium. Our prototype antenna will rest inside a cylindrical plastic tube, having the antenna surrounded by air. Also, initial plans were to have the operating frequency of the antenna be between 900 MHz to 1 GHz, but we have now increased the range of operation to 2.4 - 2.5 GHz. This provides higher resolution and allows for a much smaller antenna design, with the sacrifice being penetration depth. Penetration depth is to be improved with the implementation of an antenna array.

2.2 Subsystem Specifications

In order to transmit and receive the signal properly, the antenna must be constructed according to calculated measurements. Important elements include the length and width of the tapered slot and the diameter of the circular slot stub, located behind the coaxial feed location, as shown in figure - in section 2.4. Width is calculated to be one half of the minimum wavelength of operation, and length is calculated to be the minimum wavelength of operation. The diameter of the slot stub is calculated to be one fourth of the effective wavelength. Another vital specification is the exponential curve of the sides of the tapered slot, which is calculated in section 2.4.

Table 2.1
Antenna specification Compliance Matrix

Specification	Min	Nominal	Max
Operating Frequency	2.4025 GHz	N/A	2.4775 GHz
Length of Tapered Slot	.125 m	.126 m	N/A
Width of Tapered Slot	.0625 m	.0635 m	N/A
Diameter of Circular Slot Stub	.0306 m	.0306 m	.0306 m

2.3 Subsystem Status

Currently, an antenna surrounded by air has been constructed, except for the slot stub. The coaxial lines have been ordered, and the toroidal core for the balun is also not in-hand yet. Testing can begin the moment components come in and the cable is soldered to the antenna.

2.4 Subsystem Technical Details

A diagram of the vivaldi antenna is shown in (2.1). Note that instead of a microstrip feedline, we are soldering the conductors of a coaxial cable directly to the feed point shown in the diagram. The purpose of using a vivaldi antenna is to provide a smooth transition between the wave being guided through the slotline to the plane wave. This is made possible through the exponential curve of the slotline. The coaxial cable is soldered to where the voltage difference occurs across the slotline gap. As the signal travels across the edges, the increase in the size of the gap causes a gradual change in impedance, until the signal is matched with its surrounding medium, allowing it to propagate out of the metal. The coordinates for the curve are found using (2.1), with (2.2) and (2.3) being supplemental. The coordinate system used has the origin at the center of the coaxial feed point. This mean that, for one side of the antenna and with an initial slotline width of 2 mm, $(z_1, y_1) = (0, 1)$ and $(z_2, y_2) = (126, 31.75)$. The rate of expansion, R , should be adjusted according to how the antenna performs during testing, but as a starting point, has been set to .2 after consulting other vivaldi antenna tests. This sets C_1 at .220561 and C_2 at -.263939, making the equation used for the curvature of our antenna (2.4).

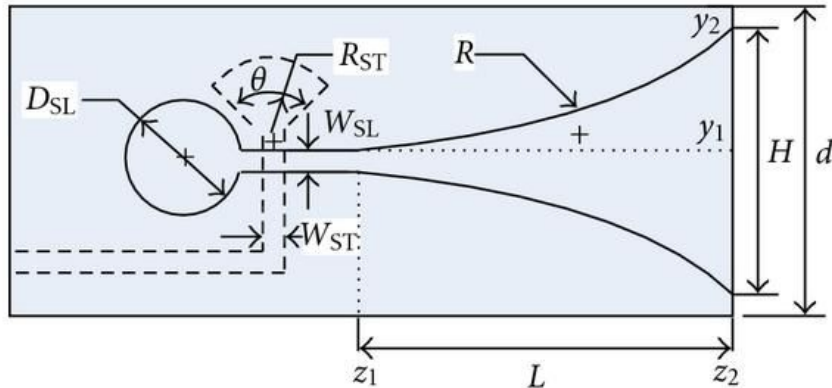


Figure 2.1: Vivaldi Antenna Diagram, with microstrip feedline

$$z = C_1 e^{Ry} + C_2 \quad (2.1)$$

$$C_1 = \frac{(z_2 - z_1)}{(e^{Ry_2} - e^{Ry_1})} \quad (2.2)$$

$$C_2 = \frac{(z_1 e^{Ry_2} - z_2 e^{Ry_1})}{(e^{Ry_2} - e^{Ry_1})} \quad (2.3)$$

$$z = .220561e^{-2y} - .263939 \quad (2.4)$$

The balun is a vital aspect of the antenna system, as directly soldering an unbalanced line such as a coaxial cable to a balanced antenna has debilitating effects. Common mode waves, where current is flowing in the same direction on both conductors of the transmission line, is undesirable because it causes the outer surface of the coaxial cable to radiate, causing power to be lost radiating in the wrong direction, which makes the antenna much less effective. For our subsystem, a 1:1 choke balun is to be implemented using a toroidal core. Before feeding into the antenna, the coaxial cable will be wrapped around the toroidal core N amount of times, preventing signals from flowing along the outer surface of the coaxial cable. The necessary amount of loops around the core, N, is expected to be 10, but can be modified if performance is not acceptable.

Vivaldi antennas generally have a gain of roughly 5-10 dBi, and we are expecting a bandwidth of about 75 MHz. The reflection coefficient at the input, S_{11} , is expected to be around .333, and is dependent on how smooth and sharp the exponential curve of the antenna is.

Table 2.2
Antenna Design

Parameter	Specification	Simulation results
Gain	5-10 dBi	-
Bandwidth	75 MHz	-
Reflection Coefficient	.333	-

2.5 Subsystem Testing

2.5.1 Validation of Antenna Specifications

The purpose of this test is to use a network analyzer to fully test the functionality of the constructed vivaldi antennas in order to verify that the specifications allow the antenna to operate at an acceptable level for the system as a whole. The major passing condition is whether the antenna is deemed able to properly emit a signal powerful enough to overcome attenuation through the ground. Specifications can be actively altered during testing until results are acceptable.

Test Setup

The input coaxial line will be fed into a network analyzer for testing. The vivaldi antenna must be facing free space with no obscurities around it. The primary results to be analyzed from the network analyzer include the reflection, the VSWR, the smith chart, and the radiation.

Data

Currently, the test has not yet been completed due to lack of physical components. Testing is to be run as

Daniel Miller, Tyler Castro, Michael Turner, Coy Coburn

Team 24 Ground Penetrating Radar

soon as the subsystem is complete.

Test Conclusion

Currently, the test has not yet been completed due to lack of physical components. Testing is to be run as soon as the subsystem is complete.

Daniel Miller, Tyler Castro, Michael Turner, Coy Coburn

3 Subsystem Receiver Circuit

The receiving circuit will take the signal obtained by the receiver antenna and amplify the signal before passing it on to the demodulator. The circuit itself will consist of a PIN diode and driver circuit, a schottky diode clamp, and an LNA (Low Noise Amplifier). The circuit diagram for the subsystem is in Appendix B.

3.1 Significant Changes in Direction

The original design of the circuit consisted of a TVG (Time Varying Gain) followed by a LNA. The TVG was removed due to the risk of it producing noise that could lead to the loss of detected objects. A PIN diode and a schottky diode clamp were added to help prevent high powered signals, that could be generated from the air to ground reflection, from damaging the LNA. A driver was added to control the switching of the PIN diode. These changes help simplify the design and construction of the receiver circuit as well as help improve its ability to handle the signal obtained by the receiver antennas.

3.2 Subsystem Specifications

In order to prepare the signal for converting, the receiver circuit must be able to amplify the signal for the demodulator while limiting the incoming signal to protect the LNA. Important elements include the LNA, the schottky diodes and the PIN Diode Driver. The specifications of the important elements are listed in Table 3.1.

Table 3.1
Receiver Circuit specification Compliance Matrix

Specification	Min	Nominal	Max
LNA Gain	15.5 dB	17.9 dB	18.9 dB
LNA Noise Figure	0.4 dB	0.5 dB	0.9 dB
Schottky Diode Forward Voltage	250 mV	340 mV	700 mV
PIN Diode Driver Switching Speed	10 ns	50 ns	100 ns

3.3 Subsystem Status

Currently the receiver has been designed and simulations using ADS (Advanced Design Software). The LNAs and the LNA eval board have arrived. The Schottky diodes and SMA cords have been ordered. The PIN diode driver needs work to improve its switching speed.

3.4 Subsystem Technical Details

The LNA is the main component of the receiver circuit as it is required to amplify the signal for the signal converter. The LNA needs a very low noise figure and must be able to handle the required frequency range of 2.4GHz. The TAV-541+ was chosen because it meets the requirements with a frequency range of

0.450 GHz to 6 GHz, a noise figure of 0.7 dB at 2.4 Ghz, and has a gain of 18 dB at 2.4 Ghz.

The schottky diodes are added to protect the LNA from high powered signals. The activation range of the schottky diode was determined to be between 1 dBm and 17 dBm. Using the equation 3.1, it was calculated that the schottky must have a forward voltage greater than 0.250 V but lower 1.5V. The 1PS70SB84 was chosen because it meets the requirements with a forward voltage of 0.340 V.

$$Voltage = \text{SQRT}((50\Omega * 1dBm) * 10^{\text{power}/10}) \quad (3.1)$$

The PIN diodes and driver were added to protect the LNA from initial air to ground reflection. The PIN diode driver must be able produce the proper forward voltage and reverse current to drive the PIN Diode. The driver must also be able to switch between forward bias and reverse bias rapidly.

3.5 Subsystem Testing

Two test will be performed for the receiver circuit. The first will test if the schottky diodes can limit high powered signals that can damage the LNA. The second will test if the PIN diode driver can successfully generate the proper forward voltage and reverse current.

3.5.1 Schottky Diodes

The purpose of this test it to determine if the Schottky diodes can protect the LNA from high powered signals. The Schottky needs to turn on when the input is between 0.250 V and 1.5 V to sufficiently prevent high powered signals from passing to the LNA. The test will pass if the Schottky diodes can activated within that range.

Test Setup

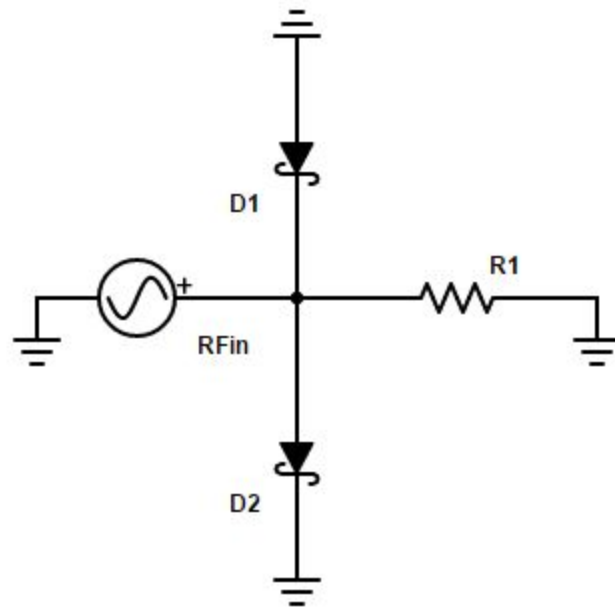


Figure 3.1 Schottky test circuit diagram

The test will be conducted in lab using the function generator, the oscilloscope, the schottky diodes (D1 and D2), and a 50Ω resistor (R1). The circuit will be set up as shown in Figure 3.1. The function generator (RFin) will generate a sine wave with a frequency of 2.4 GHz with a starting amplitude of 100 mV. A probe from the oscilloscope will be connected after the schottky diodes and measure the signal over the 50Ω resistor (R1). The amplitude of function generator will be increased until 2 V.

Data

No data has been recorded for this test setup as of now. This will change once the necessary hardware has been bought and accounted for.

Test Conclusion

No data has been recorded for this test setup as of now. This will change once the necessary hardware has been bought and accounted for.

3.5.2 PIN Diode Driver

The purpose of this test it to determine if the PIN Diode driver can produce the proper forward voltage and reverse current. The test will pass if the PIN Diode driver can properly produce the correct forward voltage and reverse current.

Test Setup

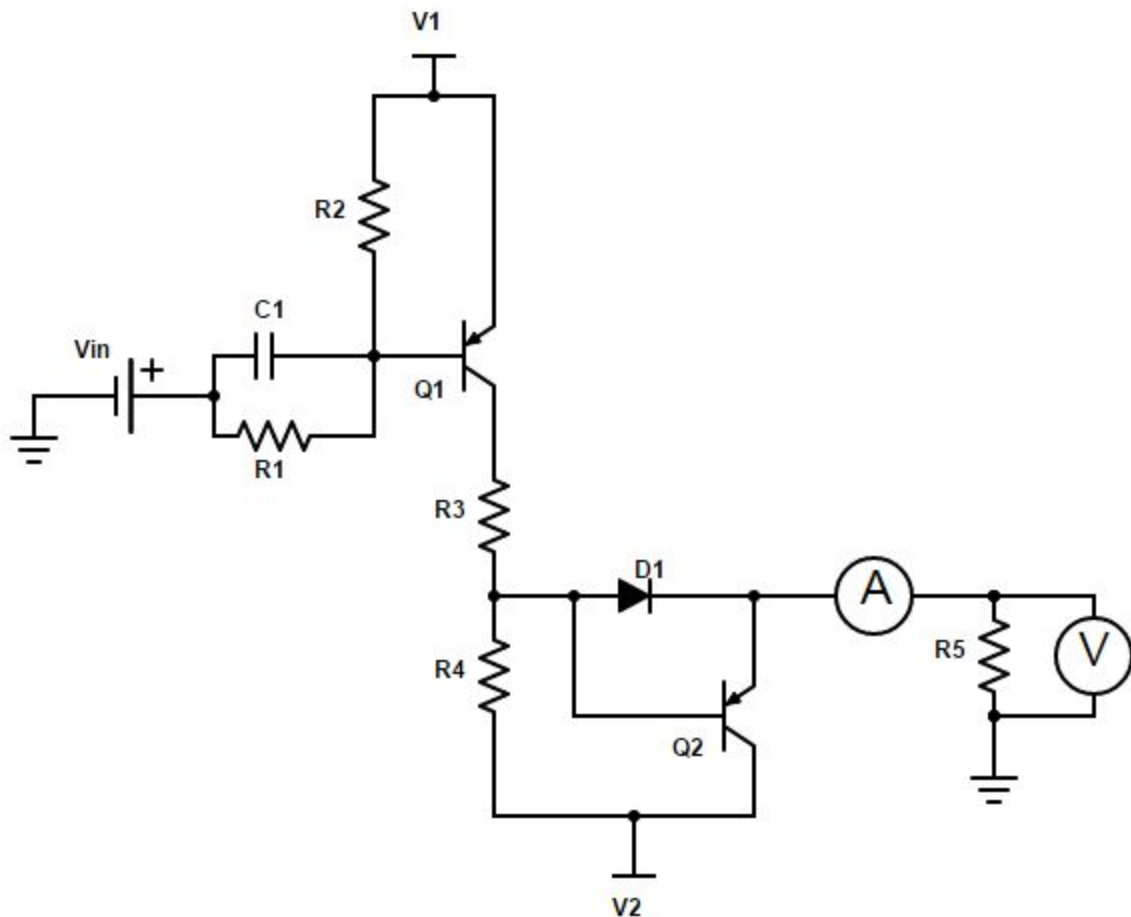


Figure 3.2 PIN diode driver test circuit diagram

The test will be conducted in lab using 3 DC power supply, a voltmeter, an ammeter, the PIN diode driver, and a 50Ω resistor (R5). The circuit will be set up as shown in Figure 3.2. The first DC power supply will be connected to V1 and set to 5V. The second DC power supply will be connected to V2 and set to 40V. The third DC power supply will be connected to Vin and set to 0V. A voltmeter will be connected in parallel to the 50Ω resistor (R5) to measure the forward voltage. Vin will be set to 5V. The ammeter will be connected in series with the 50Ω resistor (R5) to measure the reverse current.

Data

No data has been recorded for this test setup as of now. This will change once the necessary hardware has been bought and accounted for.

Test Conclusion

No data has been recorded for this test setup as of now. This will change once the necessary hardware has been bought and accounted for.

Daniel Miller, Tyler Castro, Michael Turner, Coy Coburn

Team 24 Ground Penetrating Radar

Daniel Miller, Tyler Castro, Michael Turner, Coy Coburn

4 Subsystem Signal Generation

Signal generation focuses on generating a linear frequency-modulated continuous wave. The signal will operate in the 2.4-2.475GHz ISM band. A triangular wave generated from a monolithic function generator will be passed to a voltage-controlled oscillator (VCO) that will modulate the signal frequency based directly on the voltage applied. The triangular wave's frequency and duty cycle can be modulated by resistors placed across selected terminals on the function generator. The waveform then passes through a series of power amplifiers before being propagated into the ground by the transmitting antenna.

4.1 Significant Changes in Direction

A recent significant change in direction is the shift from pulse-compression to continuous wave. This change was made to simplify the circuit and to save overall costs by avoiding SAW filters. The omittance of pulse-compression comes at cost though; range of resolution is slightly impaired and more power is needed to generate this signal. To counteract this impairment, the frequency was increased from the 915 MHz ISM band to the 2.4 GHz ISM band. The increase in frequency also means higher attenuation losses and therefore more power needed at the transmitting antenna. Overall these changes were made to simple the circuit but at the cost of more power.

4.2 Subsystem Specifications

In order to generate the correct signal, the components in table 4.1 were carefully selected to meet the desired frequency range. The next criteria for selecting the components were based on performance. An important performance parameter displayed in table 4.1 is input and output voltages as well as gain through the elements. Based on antenna sensitivity and power loss through the material a minimum of 50 mW is required at the output. The following components were selected to achieve this requirement.

Table 4.1
Signal Generation specification Compliance Matrix

Specification	Min	Nominal	Max
XR-2206 (Function Generator)(Output)	N/A	160 mV/kΩ	N/A
ZX95-2536C+ (VCO)(frequency)	2.315 GHz	N/A	2.536 GHz
VCO (input)	.5 V	N/A	5V
VCO(power)		6dBm	
	N/A		N/A
ZX60-272LN+ (PA)	N/A	14 dB	N/A

Daniel Miller, Tyler Castro, Michael Turner, Coy Coburn

4.3 Subsystem Status

The function generator and VCO are currently in the mail. Once the components arrive they will be tested and finalized following the test plan detailed in section 4.5 Subsystem testing. A power amplifier is still being considered because of the relatively high costs when operating at such high frequencies but the component detailed in table 4.1 should prove a likely candidate for the final selection.

4.4 Subsystem Technical Details

The objective of this analysis turns out to be finding the minimum required pulse duration to achieve the required range of resolution. The minimum required pulse duration can be calculated from (4.1) where d_m is the required range of resolution of 3 inches. According to (4.1) the minimum required pulse would be 1.24 ns. The monolithic function generator was selected for its frequency of over 1 MHz which satisfies the pulse duration required above.

$$\min \text{ pulse} = \frac{2*d_m}{\text{propagation velocity}} \quad (4.1)$$

$$f = \frac{2}{C} \left[\frac{1}{R_1 + R_2} \right] \quad (4.2)$$

$$\text{Duty Cycle} = \frac{R_1}{R_1 + R_2} \quad (4.3)$$

This minimum pulse is considered a percentage or duty cycle of the period (T). Working backwards from (4.3) to (4.2) with $R_1 = 100k\Omega$ as a requirement, one will find that $R_2=10k\Omega$ and $C=.01\mu\text{F}$ with $f= 1\text{MHz}$. Following the circuit displayed in appendix B, the function generator circuit, R_1 is connected across pin 7 and ground and R_2 is connected across pin 8 and ground. The capacitor is then connected across pins 5 and 6. These components will produce a triangle wave with a pulse of 1.24 ns.

The voltage controlled oscillator (VCO) was selected because its optimum frequency range between 2.315 GHz to 2.536 GHz. Voltage is directly proportional to the output frequency this means as voltage increases, so will the output frequency. According to the data sheet in order to operate within our desired ISM band and bandwidth a voltage range of 2.2-2.7 voltages will be applied. The VCO offers two soldering points so the function generator can easily be attached to the input and a coaxial output so it can be easily be connected to the power amplifiers in the next stage.

The power amplifier was selected to meet the required minimum of 50 mW. The calculation is based on antenna sensitivity(Si), tangential sensitivity(TS), power loss through the media(A), signal

reflection of ground and roots(GR), line loss (LS) and power generator by the VCO(VCO). Equation (4.4) shows the power calculation needed at the antenna.

$$Si - TS + GR + A - TS + LS + VCO = \text{power}$$

According to this equation the power amplifier needs to be greater than 11dB. By cascading several of the power amplifiers selected in table 4.1 a large power output can be achieved.

4.5 Subsystem Testing

4.5.1 VCO Output

The purpose of this test is to observe and verify the change in frequency versus time in the signal generated by the VCO. The major pass fail condition for this test is whether the frequency change spans the proper bandwidth or not, as well as if the signal period is the proper duration.

Test Setup

The output of the VCO should be connected directly to the oscilloscope using a coaxial cable and set up with the proper power level. The oscilloscope should be set up to view the resulting waveform as a function of time, and used to view the frequency according to time.

Data

Currently this test is unable to be performed due to lack of the proper materials. Once the parts are physically in hand, testing will begin.

Test Conclusion

Currently this test is unable to be performed due to lack of the proper materials. Once the parts are physically in hand, testing will begin.

5 Subsystem Receiver Signal Converter

The purpose of the receiver signal converter subsystem is to take the Rx signal and convert its wave into digital points to be used for image processing. Once the received signal has been amplified by the LNA circuit, it will then be sent through a frequency mixer to manipulate the frequency back to the frequency that was originally transmitted. A DDS will be used as the LO feed for correct matching. Once mixed, the resulting IF signal is fed to a demodulator and ADC to sample and convert the analog signal into digital values that will be recorded and saved for image processing uses.

5.1 Significant Changes in Direction

Multiple changes have been made during the production of this subsystem. Originally, a BeagleBone Black was chosen for AD conversion, however the sampling rate of a regular unit is 200 KHz, which is too low for the necessary sampling frequency needed for this circuit. Earlier requirements included processing the digital data into an image displayed on screen for the user, however the new requirement is to only record and store the digital data into easily imported files for other machines and systems to use. Finally, the phased array portion of the project was replaced with only one channel. This resulted in the circuit's need of only one mixer instead of a mixer for each channel and power combiner. The coaxial phase shifters were also removed from the subsystem due to this change.

5.2 Subsystem Specifications

The hardware needed for this subsystem must be able to work in the necessary frequency range, which is based on the bandwidth of 2.4025 – 2.4775 GHz. With this bandwidth spec, a sampling rate of 150 MHz is also needed for correct sampling based on the Nyquist theorem. With the requirement of a spatial resolution of 7.62 cm, a frequency resolution of 2.4 MHz was calculated as the requirement. Based on the prior sampling rate, about 63 samples will be taken during each rise in the triangular wave.

Table 5.1
Signal Generation specification Compliance Matrix

Specification	Min	Nominal	Max
Direct Digital Synthesizer	2.4025 GHz	N/A	2.4775 GHz
Mixer	2.0 GHz	2.4 – 2.475 GHz	2.75 GHz
Analog to Digital Converter	150 MHz	150 MHz	N/A
Demodulator	2.0 GHz	2.4 – 2.475 GHz	2.75 GHz

5.3 Subsystem Status

Hardware is currently being researched and listed in a pricing document that will be sent to the sponsor in the Geophysics department. From there, a matching will be done and the team will be given an approved budget. Given the specific and needed specs for the conversion hardware, this subsystem will be the most expensive of the project.

5.4 Subsystem Technical Details

The DDS was included into the receiver signal converter subsystem for the intended purpose to act a local oscillator for the mixer circuit. Initial plans were to install a power splitter from the transmitter circuit and send it to the mixer, but concerns on testing and possible desynchronization of the two systems led to the decision to include the DDS. The key performance specs of the DDS is the phase noise, jitter, and spurious-free dynamic range.

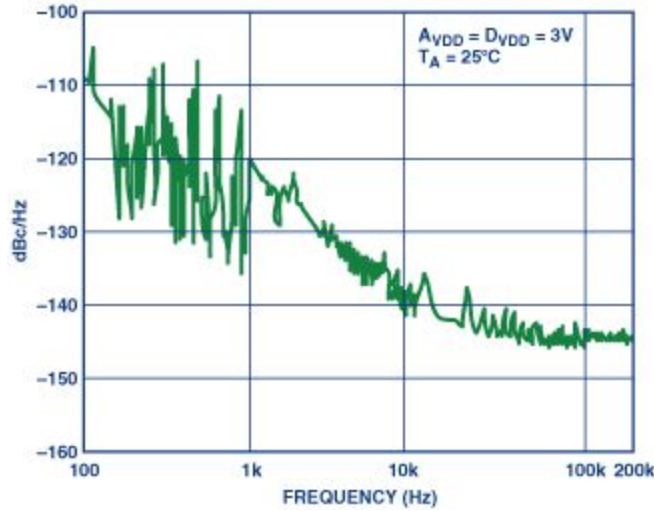


Figure 5.1. Typical output phase noise plot for the AD9834. Output frequency is 2 MHz and M clock is 50 MHz.

The mixer is fundamental in correcting any frequency change occurs in the received signal. The mixer needs to be able to work in the bandwidth range expected. The LO power into a diode mixer should be 10 dB greater than the highest input signal level anticipated. However, high-IP3 mixers can work with a LO power 3dB less than the RF power. The 1-dB compression point is used for choosing the mixer's LO power.

The demodulator needs to meet certain specs regarding the frequency range, sampling rate, and power dissipation. The sampling rate is taken from the bandwidth of the transmitted signal. The frequency range is found through the minimum and maximum frequencies that the signal will reach. The power dissipation will need to be kept to as little as possible to avoid having to change power amplification due to the increased attenuation.

The analog-to-digital converter must meet certain specifications that have been found through calculations.

$$t_{flight} = \frac{depth}{C_{sand}} \quad 5.2$$

$$slope = \frac{BW}{4*t_{flight}} \quad 5.3$$

$$f_{sampling} = 2 * BW \quad 5.4$$

$$\Delta f = \frac{2*spatial\ resolution}{C_{sand}} * slope \quad 5.5$$

$$\Delta f = 1/T \quad 5.6$$

$$T = \frac{\text{samples}}{f_{\text{sampling}}} \quad 5.7$$

These calculations can be utilized to find the necessary sampling rate and samples that will be needed for accurate conversion of the given signal. Based on a maximum depth of 1.2 m and the signal speed through sand found to be $1.22 * 10^8$ m/s, the time of flight is 9.8 ns. With a bandwidth of 75 MHz and increasing the time to 40 ns as a buffer, the slope is found to be $1.9 * 10^{15}$ Hz/s. Based on the Nyquist sampling theorem, the sampling rate must be at least equal to twice the bandwidth, which results in being 150 MHz. Frequency resolution is then found from the spatial resolution of 7.62 cm, C_{sand} , and the slope of frequency rising over time. Taking into consideration of the relation between the frequency resolution and sampling rate, the number of samples can be found. The lowest possible number of samples will be 62.5, with the ceiling resulting in 63 samples per rise. The key with the ADC is finding a unit that has the necessary sampling rate, since higher sampling frequencies also means higher cost.

5.5 Subsystem Testing

Two test will be performed. The first will test the mixer and the DDS capabilities. The second will test the demodulator and ADC.

5.5.1 Mixer induced frequency shift

This test will be testing for the accuracy of the resulting IF signal once the Rx has been mixed with the LO signal generated by the DDS.

Test Setup

The needed hardware is the DDS, the mixer circuit, wave function generator, and a network analyzer. Using frequency-offset mode, the output from the mixer will be sent directly into the reference input of the analyzer. Once specifying the measurement setup on the settings panel, the proper RF frequency span is calculated to create the needed IF frequency. Some analyzers will also sweep the source backwards to find the wanted IF span. The DDS will be utilized of the LO, which will also check its capabilities with the mixer circuit.

Data

No data has been recorded for this test setup as of now. This will change once the necessary hardware has been bought and accounted for.

Test Conclusion

No data has been recorded for this test setup as of now. This will change once the necessary hardware has been bought and accounted for.

5.5.2 Demodulation and analog-to-digital conversion

The purpose of this test is to test the reliability of the demodulator and ADC. This will be done by measuring the code transitions.

Daniel Miller, Tyler Castro, Michael Turner, Coy Coburn

Test Setup

The test will need the demodulator, ADC, analog voltage source, LED display, and a DVM. The analog source is fed through the demodulator and to the ADC circuit. The input source is varied across the possible values until the LEDs continue switching between two codes. The input voltage is recorded. Possible problems include the ADC not possessing a good PTP input-referred noise.

Data

No data has been recorded for this test setup as of now. This will change once the necessary hardware has been bought and accounted for.

Test Conclusion

No data has been recorded for this test setup as of now. This will change once the necessary hardware has been bought and accounted for.

6 Conclusions

The signal generating subsystem consists of a function generator, VCO and several cascading power amplifiers. The function generator produces a triangular waveform that can be modified by changing the selected resistor values depending on the desired pulse duration. The VCO then modulates this triangular waveform linearly increasing the frequency of a sine wave based on the input voltages. The power amplifiers then amplifies the signal to meet the required minimum 50 mW of power. The power amplifiers are very expensive so selecting a cost efficient amplifier is crucial. Once the function generator and VCO arrive in the mail, testing and finalization as well as incorporation into the transmitting antenna can begin.

The antenna subsystem has properly constructed a prototype antenna designed for wave propagation through air at a frequency between 2.4025 and 2.4775 GHz. The antenna subsystem is currently dependent on the timely construction of the baluns in order to begin testing. Once the baluns are created, the coaxial connections can then be soldered to the vivaldi antennas to begin testing using the network analyzer. Ensuring that the design for the prototype antenna is functioning properly will allow for the altering of the system to fit propagation through ground. A future design idea looking to be implemented is the change of the medium the antenna is sitting in from air to water.

The receiver circuit subsystem is in the process of buying hardware and designing the PIN Diode driver and PCBs for the circuit. Once it is all constructed and tested, it will then be integrated with the receiver antenna and receiver signal conversion to take an incoming Rx signal and test for amplified signal conversion. The main obstacle at the moment is designing a fast switching PIN Diode driver to protect the LNA from the initial air to ground reflection.

The receiver signal conversion subsystem is in the process of buying hardware and finding the necessary funding for these portions. While they were not made, the pieces will still be tested once combined together to actually create the required circuit. Once testing is passed, it will then be integrated with the receiver subsystem to actually take an incoming Rx signal and test for amplified signal conversion. Again, the main obstacle at the moment is finding the funding for the DDS, mixer, demodulator, and ADC with the required specs. Another alternative is to reduce the bandwidth to a smaller gap, which would bring the price of the ADC down. However, the drawback is that the transmitter subsystem would need to be adjusted for the change as well as redo other calculations as well.

The system is currently in the process of gathering all of the required components in order to begin testing. Once the parts are obtained, individual testing can occur, and finally the integration of each subsystem can begin. Further testing will most likely be needed during this process. Our time is constrained, so the team will need to commit extra hours in order to push the project forward at a quicker pace. However, recent progress and reviews with instructors and our sponsor are encouraging, as well as refocused the team's efforts towards our final goal.

References

- [1] Christian Wolff, "Phased Array Antenna ,," [Online]. Available at: <http://www.radartutorial.eu/06.antennas/Phased%20Array%20Antenna.en.html>. [Accessed: 2015]
- [2] Cedric Martel, "Modelling and Design of Antennas for Ground-Penetrating Radar Systems ,," Ph.D. dissertation, Dept. Elect. Eng, Univ. of Surrey, Guildford, United Kingdom, 2002.
- [3] "Ground Penetrating RADAR (GPR) (After Basson 2000) Introduction," GPR theory, 2007. [Online]. Available at: <http://www.geo-sense.com/gprmore.htm>. [Accessed: Jan-2015].
- [4] *Standard Guide for Using the Surface Ground Penetrating Radar Method for Subsurface Investigation*, Active Standard ASTM D6432, 2011
- [5] A. P. Annan, "Ground Penetrating Radar Principles, Procedures & Applications," Sensors & software Inc., Mississauga, Ontario, 2003
- [6] Bart Scheers, "Ultra-Wideband Ground Penetrating Radar, with Application to the Detection of Anti Personnel Landmines," Ph.D. dissertation, Dept. Elect. Eng, Catholic Univ. of Louvain, Louvain-la-Neuve, Belgium, 2001.
- [7] C. Allen , "Radar Pulse Compression ,," 2004. [Online]. Available at: https://www.ittc.ku.edu/workshops/Summer2004Lectures/Radar_Pulse_Compression.pdf. [Accessed: 2015]
- [8] Cedric Martel, "Modelling and Design of Antennas for Ground-Penetrating Radar Systems ,," Ph.D. dissertation, Dept. Elect. Eng, Univ. of Surrey, Guildford, United Kingdom, 2002.
- [9] "Ground Penetrating RADAR (GPR) (After Basson 2000) Introduction," GPR theory, 2007. [Online]. Available at: <http://www.geo-sense.com/gprmore.htm>. [Accessed: Jan-2015].
- [10] Standard Guide for Using the Surface Ground Penetrating Radar Method for Subsurface Investigation, Active Standard ASTM D6432, 2011
- [11] A. P. Annan, "Ground Penetrating Radar Principles, Procedures & Applications," Sensors & software Inc., Mississauga, Ontario, 2003
- [12] Bart Scheers, "Ultra-Wideband Ground Penetrating Radar, with Application to the Detection of Anti Personnel Landmines," Ph.D. dissertation, Dept. Elect. Eng, Catholic Univ. of Louvain, Louvain-la-Neuve, Belgium, 2001.

Daniel Miller, Tyler Castro, Michael Turner, Coy Coburn

Appendix A

Project Budget

Include a table listing the purchases/expenses for the project thus far, and note any known pending expenses.

Table A-1
Project Budget

Description	Quantity	Amount	Shipping	Line Total
TAV-541+ (LNA)	20	1.390	-	27.80
TB-154 (LNA Eval Boards)	4	29.950	-	119.80
LNA Shipping Cost	-	-	21.41	21.41
1PS70SB84 (Schottky diodes)	20	0.358	-	7.16
SMA FEMALE PCB MOUNT	8	3.15	-	25.20
SMA Cable 24 in	10	10.148	-	101.48
XR-2206 (Function Generator)	2	7.95	6.63	22.53
PA	1	39.95	-	39.95
VCO	1	44.95		44.95
Toroidal Core + Shipping	1	26.51	7.99	34.50
Sheet Metal	1	5.00	-	5.00
LMX2434	1	4.60		4.60
LMX2434EVAL	1	249.00	-	249.00
MACA-63H+ Mixer	10	12.15	-	121.50
Mixer Eval board	1	34.95	-	34.95

AD8346ARUZ Demodulator	1	849.39	-	849.39
ADC10DV200CISE/NOPB	1	87.55	-	87.55
TOTAL				1796.77

Appendix B

Subsystem Schematic

Function Generator Schematic

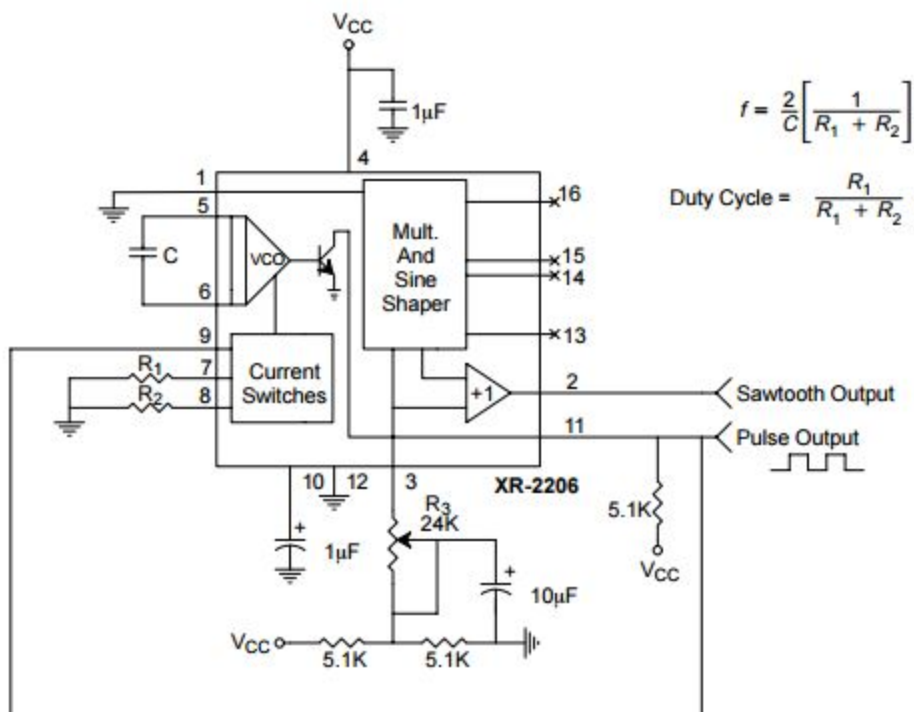


Table B-1
BOM for Signal Generation

Symbol	Value	Description
R1	100k Ω	RESISTOR, American symbol
R2	10k Ω	RESISTOR, American symbol
C	.01 μ F	CAPACITOR, American symbol
	5.1k Ω	RESISTOR, American symbol
	5.1k Ω	RESISTOR, American symbol
	5.1k Ω	RESISTOR, American symbol
	2.4k Ω	POTENTIOMETER, American symbol
	1 μ F	CAPACITOR, American symbol
	1 μ F	CAPACITOR, American symbol
	10 μ F	CAPACITOR, American symbol

Receiver Circuit Diagram

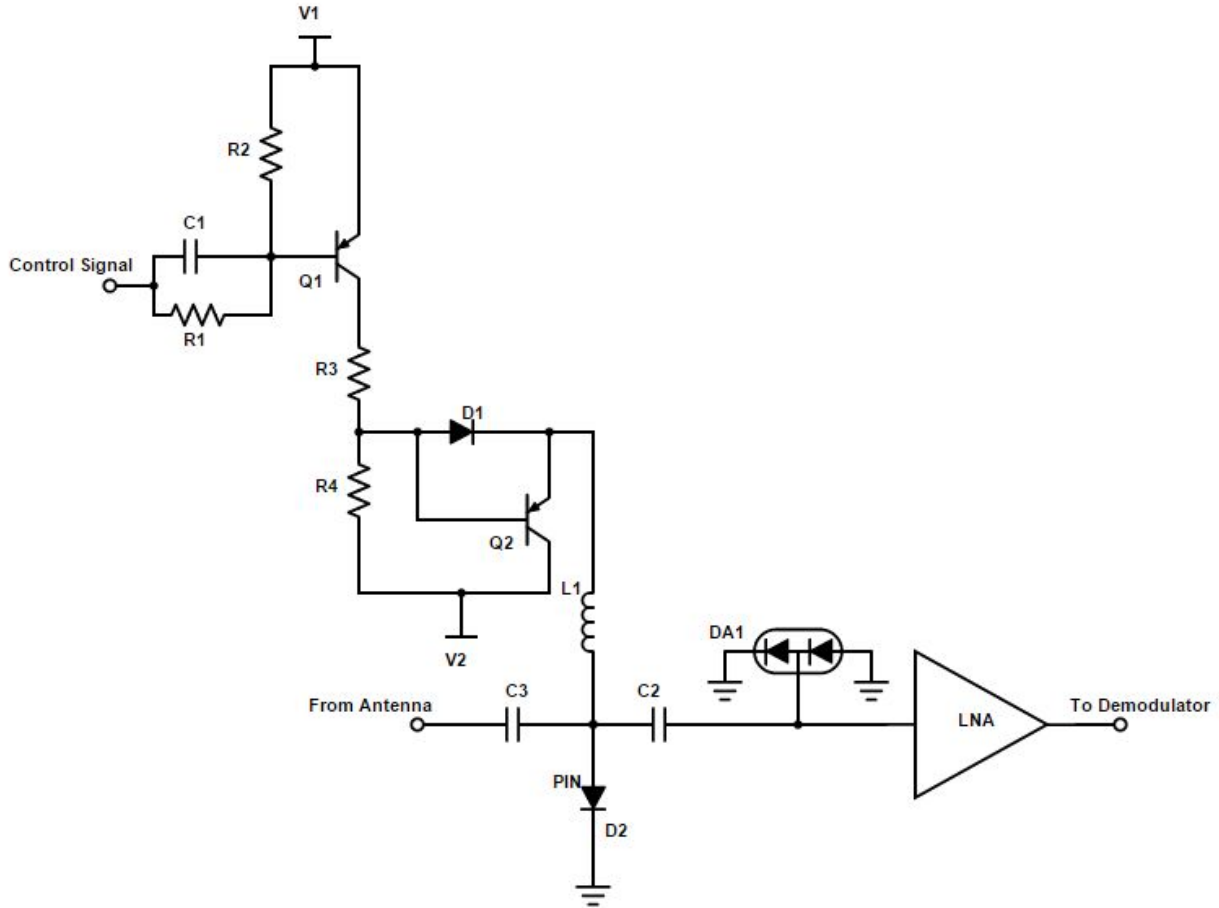


Table B-2
BOM for Receiver Circuit

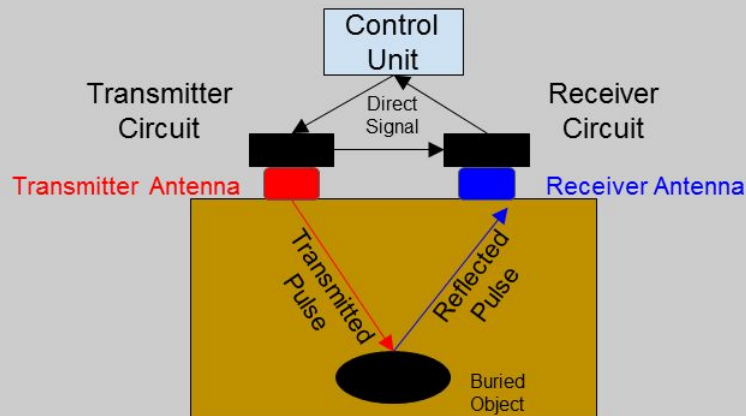
Symbol	Value	Description
R1	382 Ω	RESISTOR, American symbol
R2	955 Ω	RESISTOR, American symbol
R3	28 Ω	RESISTOR, American symbol
R4	1k Ω	RESISTOR, American symbol
C1	100pF	CAPACITOR, American symbol
C2	1μF	CAPACITOR, American symbol
C3	1μF	CAPACITOR, American symbol
L1	0.4nH	INDUCTOR, American symbol
D1	1N4007	DIODE
D2		PIN DIODE
DA1	1PS70SB82	SCHOTTKY DIODE, Series Connection
Q1, Q2		PNP Transistor
U1	TAV-541+	Low Noise Amplifier

VI - Final PPT

Team 24 - Ground Penetrating Radar

Tyler Castro, Daniel Miller, Coy Coburn, Michael Turner

Objective: To create a ground penetrating radar system to serve as a non-destructive method for mapping plant root systems

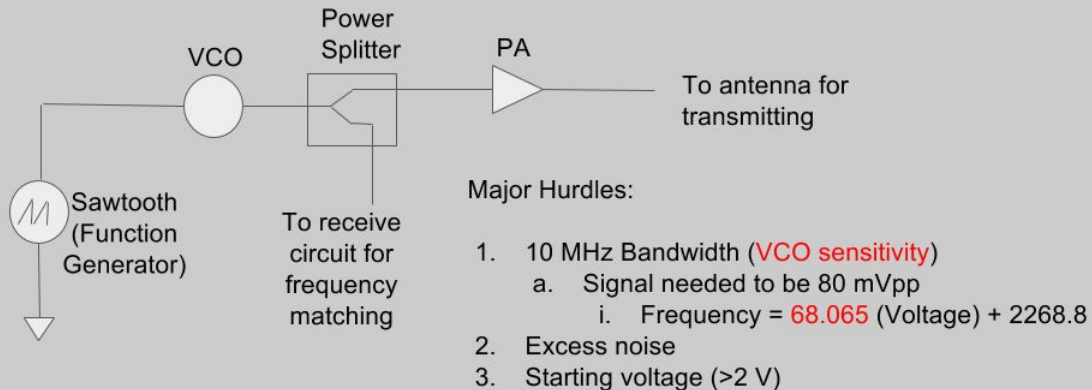


System Deliverables

- Transmitted signal will reach a ground depth of at least 0.7 m and up to 1.2 m
- The spatial resolution will be at most 7.62 cm (3 inches)
- One working channel from transmitter to receiver circuitry
- Two vivaldi antennas that are specifically designed to transmit through sand at 2.4025 - 2.4775 GHz.
- Record digital data into files that can be sent to systems for image processing

Transmitting Circuit

Daniel Miller



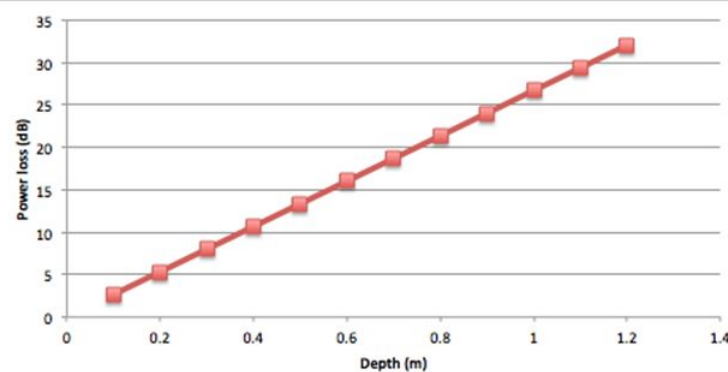
Transmitting Circuit Results

1. Output from function generator (figure 1)
 - a. 2415-2425 MHz

1. Could not test output from VCO



Transmitting Circuit - Penetration Depths



$$\alpha = \frac{2\pi}{\lambda_0} \left[\frac{1}{2} \epsilon' \sqrt{1 + \left(\frac{\epsilon''}{\epsilon'} \right)^2} - 1 \right]^{\frac{1}{2}}$$

$$P_o = P_{in} e^{-2\alpha x}$$

Sand

$\epsilon' = 6$

$\epsilon'' = 0.3$

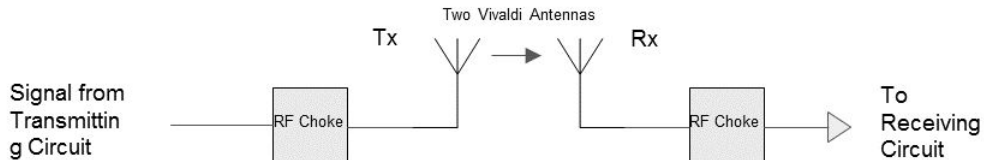
Requires minimum of -17 dBm
but will transmit 1 W

Transmitting Solutions/Improvements

1. Excess noise
 - a. Use DDS or NCO in place of function generator and VCO
2. Power output
 - a. Have several gain stages with a variable attenuator
3. Decouple power supply

Transmitting and Receiving Antennas

Tyler Castro



Major Hurdles:

1. Antennas created without substrates, which decreases cost of production, but limits reference resources available
2. Difficult to achieve a reliable connection from cable to antenna using EIC soldering materials
3. Baluns needed in order to eliminate crippling signal loss
4. Hand-made antenna ineffective from warping of metal during cutting

Antenna Results

Two versions currently created
Both cut from steel sheet metal due to very low cost
Curvature of slotline created using the following equation:
$$z = C_1 e^{Ry} + C_2$$

Version 1 (top) was cut by hand, using a rate of expansion, R, of .2
Version 2 (bottom) was cut using the EIC milling machine, with a rate of expansion of .1, and includes a radial slotline stub

Specification	Min	Nominal	Max
Operating Frequency	2.4025 GHz	N/A	2.4775 GHz
Length of Tapered Slot	.125 m	.126 m	N/A
Width of Tapered Slot	.0625 m	.0635 m	N/A
Diameter of Circular Slot Stub	.0306 m	.0406 m	.0306 m

Antenna Solutions

Testing of version 1 revealed almost complete reflection of the signal, due to:

Antenna sides no longer being coplanar from warping during cutting (solved through mill cutting)

Unreliable connection using soft solder

To achieve a solid connection for version 2:

Switch to a hard solder that can bind to steel

To prevent current flow on the outside of the coaxial cables:

Two RF chokes act as baluns for
the antennas

Coiled cables around ferrite cores act
as inductors, creating reactance along
the outer edge of the cable, preventing
current flow



Antenna Solutions

Testing of version 1 revealed almost complete reflection of the signal, due to:

Antenna sides no longer being coplanar from warping during cutting (solved through mill cutting)

Unreliable connection using soft solder

To achieve a solid connection for version 2:

Switch to a hard solder that can bind to steel

To prevent current flow on the outside of the coaxial cables:

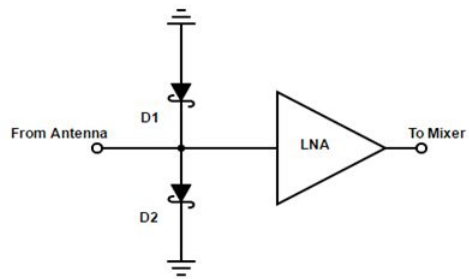
Two RF chokes act as baluns for
the antennas

Coiled cables around ferrite cores act
as inductors, creating reactance along
the outer edge of the cable, preventing
current flow



Receiver Circuit

Team member: Michael Turner

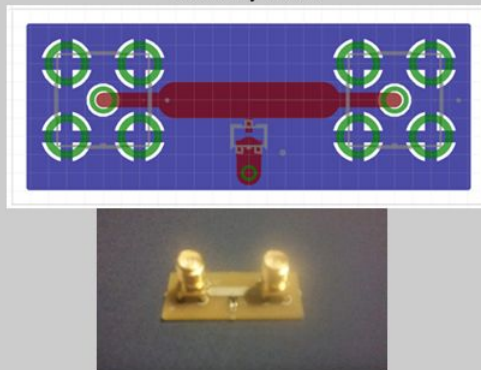


Major hurdles:

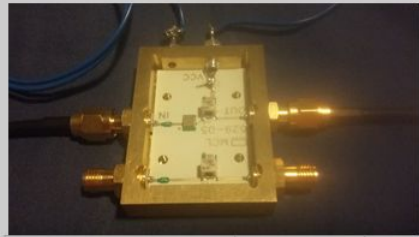
- Original design over complex
 - Originally 4 channels planned
 - PIN diode shunt switch and driver removed
- Problems with ordering parts
- Couldn't easily test circuit
 - Advanced Design System couldn't simulate several stages properly
- Lack of initial knowledge about RF led to many mistakes

Results and Solutions:

Schottky diode

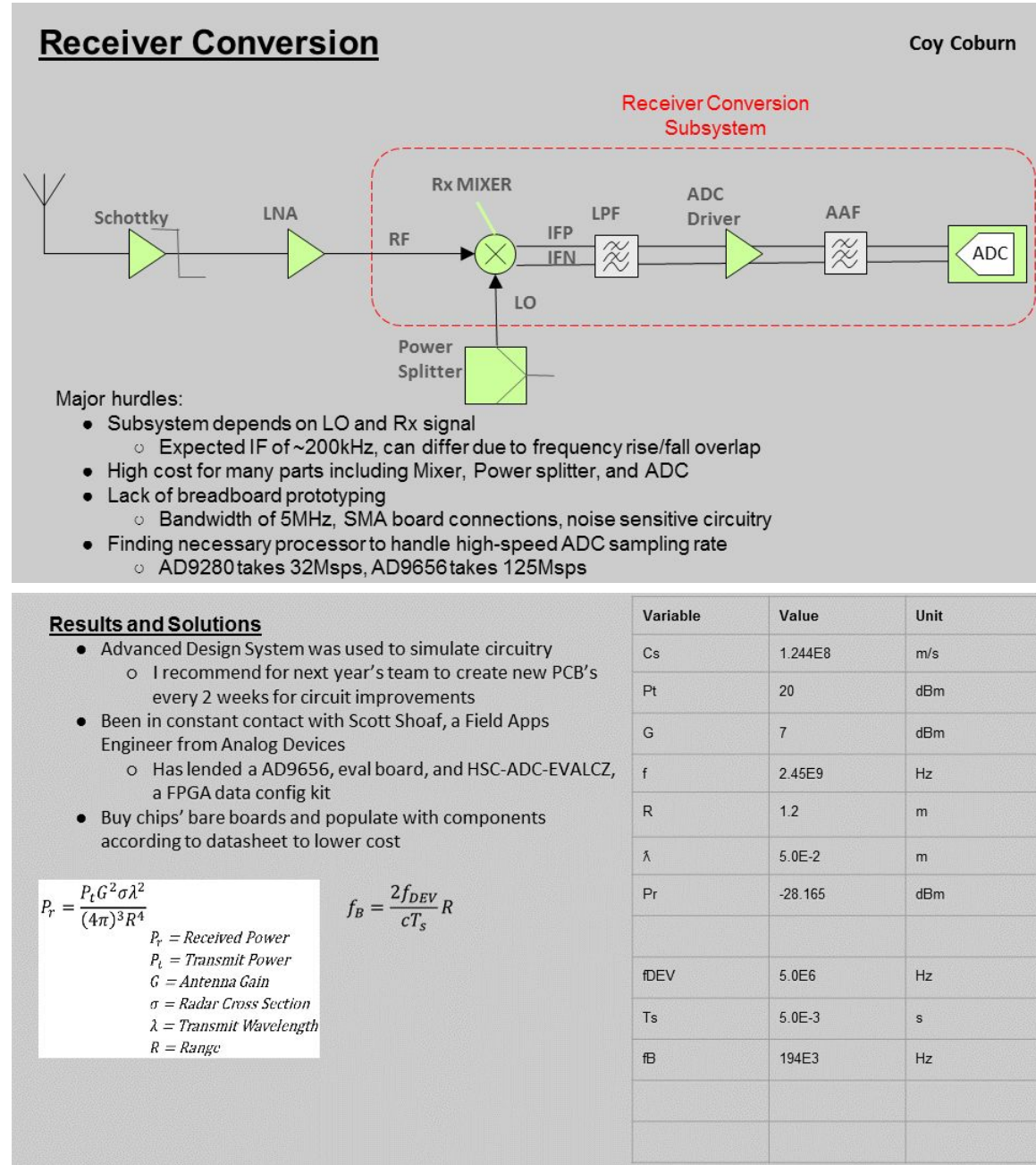


LNA



Variable	Value	Unit
Forward Voltage	700	mV
Diode capacitance	1	pF

Variable	Value	Unit
Frequency Range	0.05 - 4	GHz
Gain	13.3	dB
Noise Figure	0.95	dB
Output @ 1db	20.7	dBm
Max Input Power	17	dBm



Mixer stage board				LPF and AAF stages board			
Variable	Value	Unit	Source set	Variable	Value	Unit	Source set
ADC bits	8			$f_c = \frac{1}{2\pi RC}$	$\frac{V_o}{V_i} = (1 + \frac{R_{feedback}}{R_{GND}})$		
Resolution	256	bits		R	33	Ω	
Resol %	0.00390625	%		C	18	nF	
Vo Range (3VDD)	2.9	V		fc	267	kHz	
Vo Range (5VDD)	4.4	V		Rfeedback	1.5	k Ω	
Voltage diff level	0.01132812	5 V	3VDD	Rgnd	1.0	k Ω	
Voltage diff level	0.0171875	V	5VDD	Vo/Vi	1.5	dB	

Conclusion

While unable to completely reach our intended results, each subsystem has been calculated and established in accordance with our simulations.

Our work this semester provides a solid foundation for the next team who decides to continue this project.

Continuing on, additional improvements can be made to each subsystem, integration needs to be completed, housing for components needs to be created, and additional parts are needed to process the samples (ADC and FPGA).

Ground Breakers
Team 24
Final Report

ECEN 404 – Capstone (Senior) Design Project

Texas A&M University, College Station, TX

Daniel Miller
Tyler Castro
Michael Turner
Coy Coburn

Abstract

The goal of this project is to create a ground penetrating radar system to serve as a non-destructive method for mapping plant root systems. The system consists of a transmitting and receiving antenna and circuitry for both the transmitter and receiver. The transmitting circuit generates a linear frequency-modulated continuous wave from 2.415- 2.425GHz. The wave is pulsed to avoid interference between the transmitting and receiving antenna. The transmitting antenna passes the generated signal into the ground while the receiving antenna collects the reflected signal. The signal will reflect off materials with different dielectric constants like that of roots and pipes. The received signal will then be sent through an LNA for amplification to balance any loss of gain. The signal is also fed into a frequency mixer to correct any occurred frequency shift. Finally, the IF signal is converted into digital data that will be recorded for image processing.

Table of Contents

Abstract

Table of Contents

1 Project Overview

- 1.2 Final System Design
- 1.3 Project Deliverables
- 1.4 Task Ownership

2 Final System Status

- 2.1 Final System Performance
- 2.2 Final System Standards and Constraints
- 2.3 System Performance Improvements

3 Subsystem Transmitting Circuit

- 3.1 Significant Changes in Direction
- 3.2 Subsystem Status
- 3.3 Subsystem Challenges and Solutions
- 3.4 Subsystem Technical Details
- 3.5 Subsystem Testing

4 Subsystem Transmitting and Receiving Antennas

- 4.1 Significant Changes in Direction
- 4.2 Subsystem Status
- 4.3 Subsystem Challenges and Solutions
- 4.4 Subsystem Challenges and Solutions
- 4.5 Subsystem Technical Details
- 4.6 Subsystem Testing

5 Subsystem LNA and Receiver Protection

- 5.1 Significant Changes in Direction
- 5.2 Subsystem Status
- 5.3 Subsystem Challenges and Solutions
- 5.4 Subsystem Technical Details
- 5.5 Subsystem Testing

6 Subsystem Receiver Conversion

Daniel Miller, Tyler Castro, Michael Turner, Coy Coburn

- [6.1 Significant Changes in Direction](#)
- [6.2 Subsystem Status](#)
- [6.3 Subsystem Challenges and Solutions](#)
- [6.4 Subsystem Technical Details](#)
- [6.5 Subsystem Testing](#)

[7 Conclusions](#)

[References](#)

[Appendix A Budget Table](#)

[Appendix B Subsystem Schematic and BOM](#)

- [B-1 Function Generator Circuit](#)
- [B-2 Antenna Version 2 SOLIDWORKS Drawing](#)
- [B-3 LNA Eval Board Schematic](#)
- [B-4 Low Pass Filter and Anti-alias Filter PCB Schematic](#)

1 Project Overview

1.1 Final System Design

1.1.1 Problem Statement

Ground penetrating radar systems have been used and commercially sold since the 1980's. Since then technology has improved greatly and so has the resolution and techniques used. Geophysicists are now interested in adapting and using this existing technology to detect and measure plant root growth over a period time in a non-destructive way. Current GPRS use low frequencies in order to achieve better penetration depths. This however means that the signal passes through roots without being detected.

1.1.2 Proposed Solution

The proposed solution for geophysicists is to design a GPRS using higher frequencies. Although high frequencies are severely attenuated through media, they reflect more power off objects with different dielectric constants like that of roots. Geophysicists are only interested in the biozone approximately .7-1.2 meters in depth so the lack of penetration depth with improved resolution is highly desirable. The designed solution will utilize the 2.4025-2.47725 GHz ISM band. Since plant roots are the subject of interest a spatial resolution of 3 inches is needed.

1.1.3 Background

When comparing with current GPR systems on the market today, the primary differences from our project include the very high cost, and the fact that most commercial systems are not used for finding organic matter. The primary uses for GPR right now is concrete evaluation, where the ground is scanned for hidden piping, tunnels, or weak points in structure, in order to confirm that the area is safe for construction. Examples include the GSSI StructureScan Standard, with a penetration depth of 18 inches, operating at 1.6-2.6 GHz, used to locate rebar, PVC and metal conduits, the MALA GroundExplorer, with an operating frequency varying from 80 MHz to 750 MHz, used for deep scanning, and the GSSI SIR 3000, compatible with GSSI antennas from 200 to 2600 MHz. None of these products are aiming for root mapping purposes. Pricing for these units start at \$5000, and can go beyond the \$10000 mark.

1.2 Final System Design

The GPRS consists of a transmitting circuit, a transmitting and receiving antenna, and a receiving circuit. The transmitting circuit produces a linear-frequency modulated waveform from 2.415-2.425 GHz. This signal is passed through antennas and aimed into the ground. As the signal propagates through the ground it will reflect off objects with different dielectric constants like roots. The reflected signal is then collected using a separate receiving antenna. The receive circuit amplifies the signal and converts the signal into an easily read graph using an ADC and computer software.

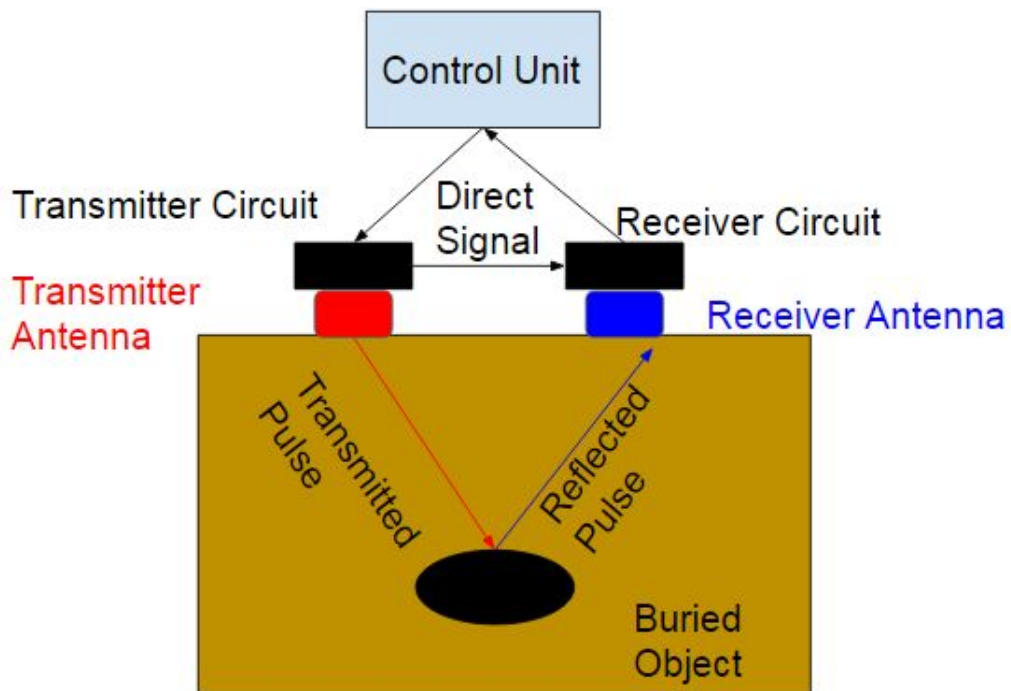


Figure 1.1: System block diagram.

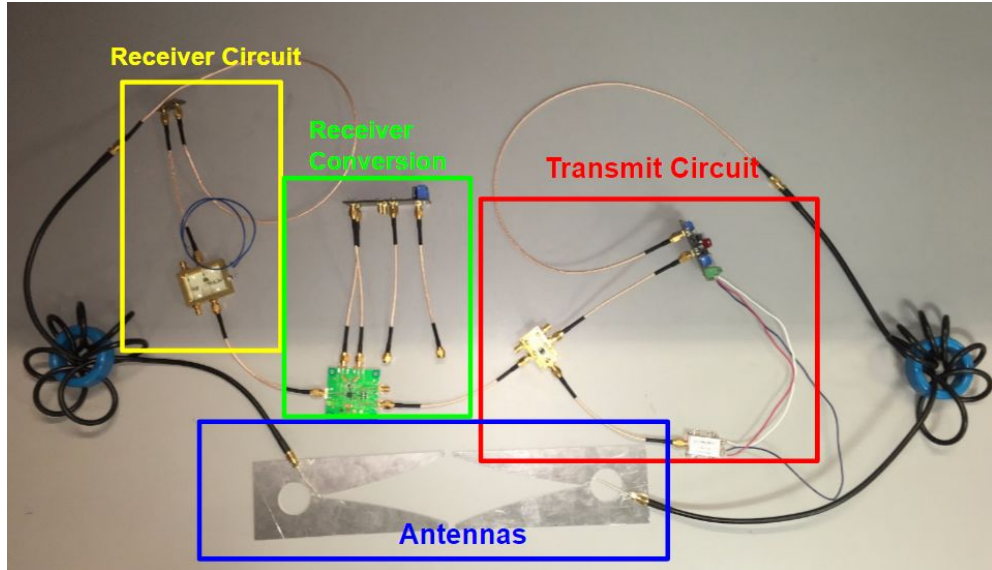


Figure 1.2: Annotated picture of system.

1.3

Project Deliverables

This section should explain exactly what the team produced. Emphasize what the team generated or developed, especially those components (HW or SW) developed “from scratch.” If system components (HW or SW) were purchased or downloaded, clearly identify these components and the team’s modification of such components to obtain the final system. Emphasize the functional requirements of the system (what the system does) and how the “end user” benefits from the system (what the end user gets).

1.3.1 Project Specifications

The transmitted signal will reach a ground depth of at least 0.7 m and up to 1.2 m. The spatial resolution will be at most 7.62 cm (3 in). There will be at least one working channel from transmitter to receiver circuitry through vivaldi antennas. These two vivaldi antennas will be specifically designed to transmit through sand with a dielectric constant of 6 at a frequency from 2.4 - 2.475 GHz. Once the received signal has been converted into digital form, the data will be recorded and stored into files that can be sent to systems for image processing.

Table 1.1
Specification Compliance Matrix

Specification	Min	Nominal	Max
Ground Depth	.7 m	-	1.2 m
Spatial Resolution	-	-	7.62 cm
Operation Frequency	2.4025 GHz	-	2.47725 GHz

1.4

Task Ownership

Tyler Castro is responsible for the design and construction of antennas that are able to operate properly in the frequency range required of the system. He will also test the antennas using a network analyzer to determine optimal specifications. Daniel Miller is responsible for signal generation. He calculated the power loss through the media and estimated the amount of power needed at the output of the antenna as well as throughout the transmitting circuit. Michael Turner is responsible for the design and construction of the receiver circuit. The receiver circuit must be able to amplify the signal obtained from the receiver antenna and pass it to the receiver signal converter while protecting itself from high power spikes that may damage the receiver. Coy Coburn is responsible for the design and construction of the receiver circuit that will mix, filter, and convert the received analog signal into digital data.

Table 1.2
Responsibility Matrix

Subsystem	Responsible Member	Responsibilities
Daniel Miller, Tyler Castro, Michael Turner, Coy Coburn		

Daniel Miller, Tyler Castro, Michael Turner, Coy Coburn

Team 24 Ground Penetrating Radar

Transmitting circuit	Daniel Miller	Design and build the transmitter circuit for the generated signal.
Transmitting and Receiving Antennas	Tyler Castro	Design and build antennas, and optimize performance.
LNA and Receiver Protection	Michael Turner	Design and build the receiver circuit that will amplify the incoming signal while limiting power spikes to protect the receiver.
Receiver signal converter	Coy Coburn	Design and build the receiver circuit that will mix and filter the incoming signal.

1.5

ABET Constraints

In order for the design to meet legal constraints, the design must follow the National Telecommunications & Information Administration's (NTIA) frequency allocation chart. According to the NTIA the industry, scientific, and medical (ISM) frequency band is openly available for use of applications of this project's nature. For that reason the available choices in frequency ranges included the 902-928 MHz and the 2.4025-2.4775GHz. The later of the frequency ranges were chosen for technical reasons.

Daniel Miller, Tyler Castro, Michael Turner, Coy Coburn

2 Final System Status

Because this project is to be continued over to the next year, our subsystems were never able to be tested together as a whole. Individual subsystems were constructed and connected together, but due to difficulty in obtaining testing equipment that operated within our frequency range, as well as troubles connecting the antennas to the systems, fully integrated testing was not possible.

2.2

Final System Performance

The system is currently not fully integrated and tested, and therefore has no results for final system performance. The system is to be completed by another group in the following year. The planned test conditions were to have three scenarios, where an empty PVC pipe, a PVC pipe filled with water, and a pipe filled with salt water were all buried in a sand pit. The water in the pipes was meant to replicate a root, as the organic matter that is plant root is primarily water. The pit needs to be deep enough to where received signals are not simply the transmitted signals hitting and reflecting off the bottom of the container/pit. This ensures that the only possible received signal reflected from the pipe.

2.3

Final System Standards and Constraints

Any root that the system is attempting to locate cannot be any more than 1.2 meters deep. The medium that the system is trying to propagate into is also a major constraint, as currently the system is designed to only propagate through sand, due to its low attenuation. It is unknown how the system will act in different ground types, but it is known that the presence of water in the ground will hamper its performance greatly.

2.4

System Performance Improvements

Multiple changes were made over the course of this project's scope. Changes in requirements, frequency, and architecture were all done and can be further improved as well.

The transmitting circuit can be improved upon by using components to greatly reduce the noise produced from the function generator. A DDS would greatly improve this noise but at a much higher price. This would ultimately affect the resolution as well depending on the clock rate of the DDS. Another further improvement to the transmitting circuit is to add cascading power amplifiers with a variable attenuator. This would allow for a variable power output from the antennas in case more power is needed based on the type of soil. A more sophisticated improvement for the transmitting circuit would be to implement pulse compression. This as well would affect the resolution but would ultimately save power.

The initial material to be used for the construction of the antennas was steel due to its low cost and easy availability. This lead to difficulties in connecting the cables to the antennas, as typical soldering techniques are not compatible with steel, and are nearly impossible with aluminum. The material determined to be the best choice is copper, because of its high conductance, which allows for higher gain on the antenna. The tradeoff here is price, but a properly working antenna is worth the higher cost. After being reviewed by peers, the rate of expansion of the expanding slot was altered in order to provide a

Daniel Miller, Tyler Castro, Michael Turner, Coy Coburn

Team 24 Ground Penetrating Radar

smoother transition into the higher impedance. The previous version of the antenna's change was determined to be too abrupt and would cause unnecessary reflection.

The receiver protection and LNA changed significantly from its original design last semester. The number of channels were decreased down to 1 to decrease the complexity of the overall system. The PIN diode was added to protect the LNA from the power spike produced by air to ground interference. It was later removed because of the complexity of its driver and the change in the way the transmitting signal was generated would cause problems with timing it's switching to remove the spike caused by the air to ground interference. Finally a schottky diode clamp was added to protect the LNA from any unintended power spikes. The only part that was not removed or changed was the LNA as it is need to amplify the received signal before passing it on to the mixer.

The receiver converter subsystem saw an overhaul in how the incoming signals were manipulated and to be converted. The power splitter in the transmitter subsystem sent one of its outputs to the mixer's LO input. This avoided the need for a DDS and greatly reduced cost. The demodulator was also removed from the system since the transmitter subsystem also removed its modulation as well. Differential outputs were updated over single-ended outputs to protect against noise and spurs in even-order harmonics. Filters and ADC driver were made to each have a gain output instead of introducing a gain amplifier block. The ADC is now needed with a FPGA data configuration board to evaluate the new digital signal and allow for software implementation during the signal processing. Further improvements can be made in impedance matching all blocks without terminating resistors as well as further subsystem testing for noise level and actual IF signal manipulation.

PCB boards were only made in the last couple of weeks during this project. This slowed testing progress and limited updates and redesigns to PCBs. Recommendation would be to create new PCBs every 2 weeks for further testing as well as improvement in design.

Necessary RF equipment for testing purposes proved to be difficult to acquire. Recommendation would be to seek equipment from Texas A&M staff and researchers to lend, with an early contract and tutorials to ensure proper usage and easy access. Continue to use ADS for early simulations and begin with tutorials before actual GPR project.

RF mentors are a highly helpful source but in short supply. Recommend to contact RF engineer and create strong connection during designing process. Also recommend to ask for RF engineer as teacher assistant for project as well.

3 Subsystem Transmitting Circuit

Signal generation focuses on generating a linear frequency-modulated continuous wave. The signal will operate in the 2.4-2.475GHz ISM band. A triangular wave generated from a monolithic function generator will be passed to a voltage-controlled oscillator (VCO) that will modulate the signal frequency based directly on the voltage applied. The triangular wave's frequency and duty cycle can be modulated by resistors placed across selected terminals on the function generator. The waveform then passes through a series of power amplifiers before being propagated into the ground by the transmitting antenna.

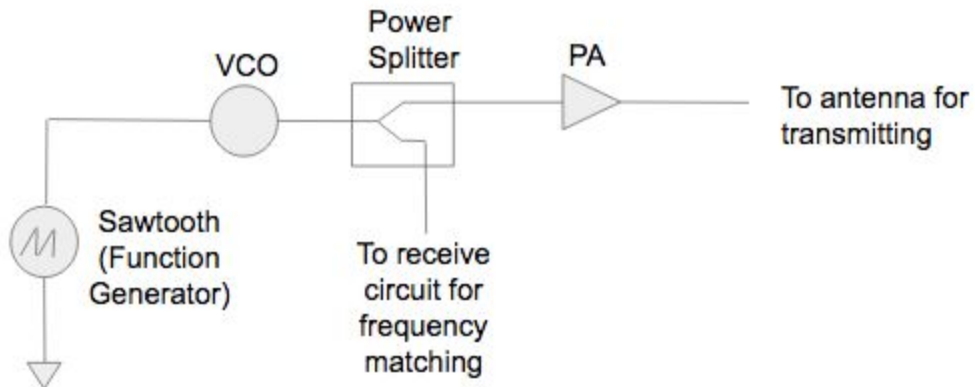


Figure 3.1: Transmitting block diagram

3.2 Significant Changes in Direction

A recent significant change in direction is the shift from pulse-compression to continuous wave. This change was made to simplify the circuit and to save overall costs by avoiding SAW filters. The omission of pulse-compression comes at cost though; range of resolution is slightly impaired and more power is needed to generate this signal. To counteract this impairment, the frequency was increased from the 915 MHz ISM band to the 2.4 GHz ISM band. The increase in frequency also means higher attenuation losses and therefore more power needed at the transmitting antenna. Overall these changes were made to simplify the circuit but at the cost of more power.

3.3 Subsystem Status

In order to generate the correct signal, the components in table 4.1 were carefully selected to meet the desired frequency range. The next criteria for selecting the components were based on performance. An important performance parameter displayed in table 4.1 is input and output voltages as well as gain through the elements. To avoid complicated calculations, only the antenna sensitivity, air to ground reflection, and power loss through the media were used to determine a minimum of 50 mW is required so the signal could be detected on the received side. This however is a rough estimate due to lack of spreading loss and other unknown factors. For this reason, the power amplifiers selected will reach the maximum output power of the ISM band which is 1W.

Table 3.1

Transmitting Circuit Specification Compliance Matrix			
Specification	Min	Nominal	Max
XR-2206 (Function Generator)(Output)	N/A	160 mV/kΩ	
ZX95-2536C+ (VCO)(frequency)	2.315 GHz	N/A	2.536 GHz
VCO (input) (power)	.5 V N/A	N/A 6dBm	5V N/A
Gain Block (gain) (P1dB)	N/A N/A	20dB 24dBm	N/A N/A

3.4 Subsystem Challenges and Solutions

There were two main challenges faced in this subsystem. A requirement proposed due to the receive side component limitations was a 5 MHz bandwidth. Due to the high MHz/Voltage sensitivity of the VCO selected, the peak-to-peak voltage needed to be 80 mVpp. This was complicated because the function generator had internal limitations that would limit the peak-to-peak voltage to around 800 mVpp. In order to achieve the 80 mVpp a voltage divider was added. Using a potentiometer, the Vpp can now be varied to meet the desired bandwidth. Another main challenge faced in this subsystem was to stay within the required ISM band. In order to meet this requirement a summing amplifier was added after the voltage divider. The summing amplifier added a DC bias to signal in order for the starting frequency to start within the ISM band.

3.5 Subsystem Technical Details

A linear frequency modulated waveform is generated using a function generator and a Voltage Controlled Oscillator (VCO). This type of waveform is generated so that the frequency domain can be utilized versus the time domain. This is important in that as a signal passes through different media, the frequency of the signal remains constant. This allows the frequency to be matched on the received side so that time and amplitude can then be measured more accurately versus the time domain.

The function generator is wired according to the circuit depicted in Appendix B. Potentiometers were used for the R1 and R2 values so that the signal's rise and fall times can be manipulated. A voltage divider and

Daniel Miller, Tyler Castro, Michael Turner, Coy Coburn

an op amp were added after the output in order to achieve several requirements discussed below. This signal is then passed to the VCO.

The voltage controlled oscillator (VCO) was selected because its optimum frequency range between 2.315 GHz to 2.536 GHz. Voltage is directly proportional to the output frequency, this means as voltage increases, so will the output frequency. Equation (3.1) was derived from the data points available on the data sheet. This equation shows that in order to start the frequency within the ISM band, a minimum of 2 volts is needed. A 10 MHz bandwidth is also required due to component limitations on the receive side. Equation (3.1) also shows that the VCO has a sensitivity of 68 MHz per volt. This means an 80 mV peak-to-peak is required to satisfy this bandwidth.

$$\text{Frequency} = 68.065 * (V) + 22268.8 \quad (3.1)$$

The power amplifier was selected to meet the required minimum of 50 mW. The calculation is based on antenna sensitivity(S_i), power loss through the media(A), signal reflection of ground and roots(GR), line loss (LS) and power generator by the VCO(VCO). Equation (3.2) shows the power calculation needed at the antenna.

$$S_i + GR + A - TS + LS + VCO = \text{power} \quad (3.2)$$

According to this equation the power amplifier needs to be greater than 11dB. This however is a rough estimate because it does not incorporate scattering losses. The power amplifier selected will provide approximately 1W at the antenna. This increase in power will ensure a strong signal will be detected at the receiver antenna.

3.6 Subsystem Testing

3.6.1 Function Generator Test

The purpose of this test is to verify the function generator operates within the requirements discussed above in section 3.3. The requirements for the signal are a starting voltage of at least 2 volts and a peak-to-peak voltage of 80 mV.

Test Setup

A DC power supply machine will be used in order provide the specific power supplies needed. Using the screw headers attached to the PCB the following power supplies will produce a signal meeting the above requirements.

Function generator power: 10V

Op-amp power: +/-15V

OP DC(for DC offset)=1.8V

An oscilloscope is than attached to the output pin of the Op-Amp. The potentiometers across R1 and R2 can be varied to order to produce the desired signal.

Data

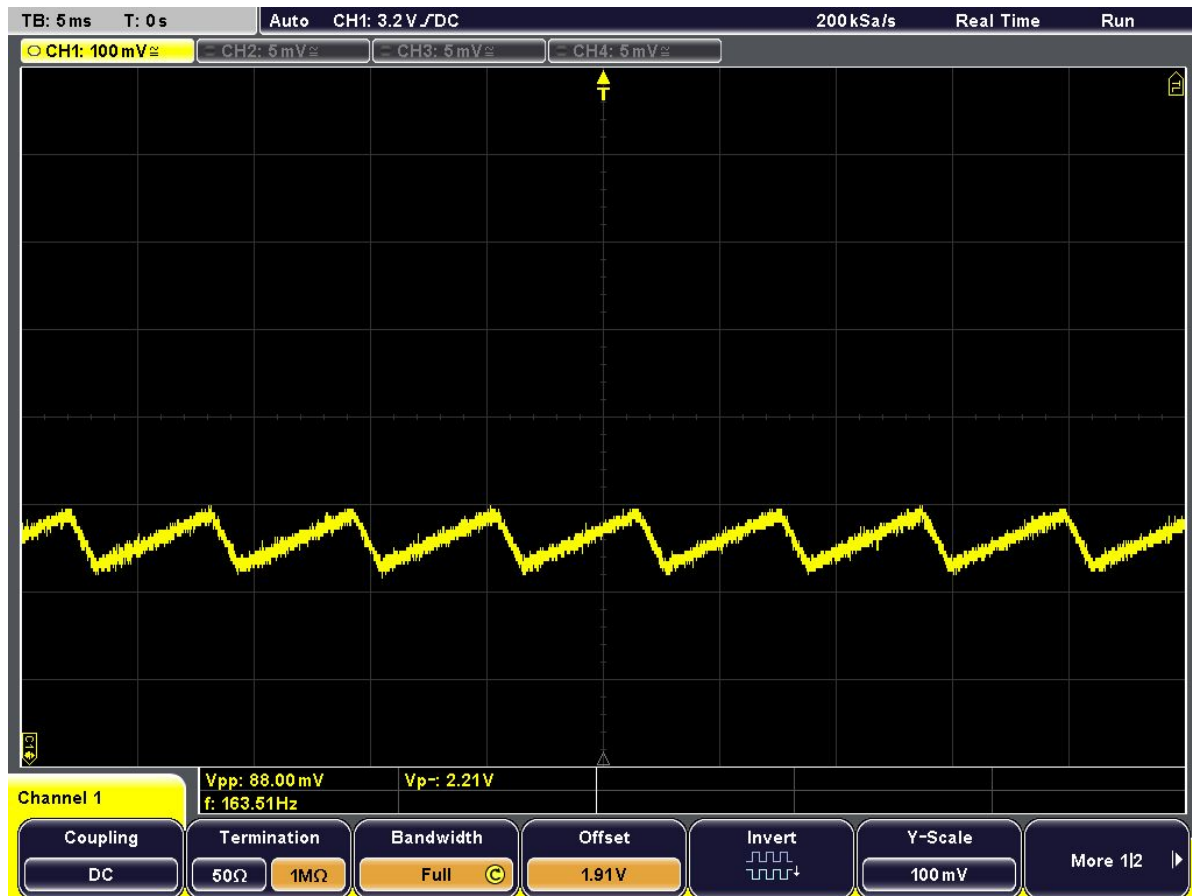


Figure 3.2: is taken from an oscilloscope with the above values.

This output shows a peak-to-peak voltage of 88 mV with a starting voltage of 2.21V. This means the VCO should operate between 2.415-2.420 GHz.

3.6.2 VCO test

The purpose of this test is to verify the VCO operates with the desired specifications and within the legal ISM band (2.4-2.4835 GHz). Unfortunately no test equipment was available to verify the results.

Test Setup

In order to test the VCO, the three input wires need to be wired accordingly. A DC power supply will be used to provide the logic power to the VCO through the VCC pin (5V). The Vtune pin is the input pin in which controls the output frequency. This pin is also connected to a DC power supply. Starting at 1V the power supply will be linearly increased by .1V intervals in order to prove equation (3.1). The ground pin must then be connected to the ground pin of the power supply. Using a coaxial cable, a spectrum analyzer will be connected in order to measure the output frequency.

Daniel Miller, Tyler Castro, Michael Turner, Coy Coburn

Another test should be performed in order to test how the function generated signal affects the VCO. This test is needed because of the noise produced from the signal generating circuit. In order to test this the function generator should be setup the same way as in the previous step (the power amplifier should be bypassed in order to avoid damaging the spectrum analyzer). A spectrum analyzer will be used again to measure the output frequency.

Data

No data is available for this section.

Conclusion

Theoretically the VCO should operate in according with the data sheet and prove (3.1). Since no spectrum analyzer was available to test how the function generator's noise would affect the output from the VCO, it will be assumed that the noise will have little to no effect.

4 Subsystem Transmitting and Receiving Antennas

The antennas are responsible for both propagating the signal generated by the transmitting subsystem into the ground, as well as receiving the reflections of the signals that reflect off of objects in the ground. The current design has a single transmitting and a single receiving antenna. An array of antennas will be implemented once a single channel is proven to be working. An input signal will be fed into a balun that will prevent current from flowing along the outside of the unbalanced coaxial cable once it reaches the balanced antenna. The output of the balun will be soldered to the sides of a vivaldi antenna, cut from sheet metal and placed in a plastic tube with measurements calculated for a frequency propagation between 2.4 - 2.5 GHz, which will be pointed to the ground. Reflections from objects buried underground will be picked up by another antenna, also connected to a coaxial cable that will serve as the input to the receiving subsystem.

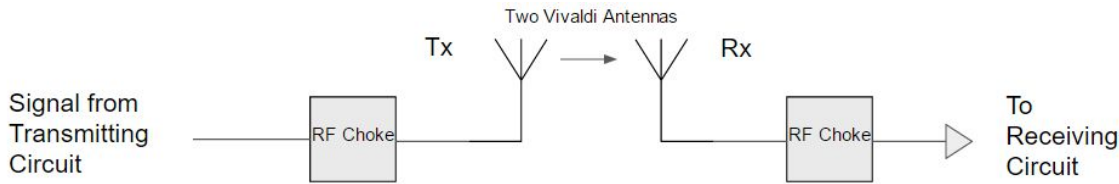


Figure 4.1: Antenna Subsystem Block Diagram

4.2 Significant Changes in Direction

The Antenna Subsystem was created rather recently, as joint efforts were previously being made to create a working transmitting system. The main change in direction is that the antenna is no longer planning to be mounted to a substrate, but rather be suspended in a medium. Our prototype antenna will rest inside a cylindrical plastic tube, having the antenna surrounded by air. Also, initial plans were to have the operating frequency of the antenna be between 900 MHz to 1 GHz, but we have now increased the range of operation to 2.4 - 2.5 GHz. This provides higher resolution and allows for a much smaller antenna design, with the sacrifice being penetration depth. Penetration depth is to be improved with the implementation of an antenna array.

4.3 Subsystem Status

In order to transmit and receive the signal properly, the antenna must be constructed according to calculated measurements. Important elements include the length and width of the tapered slot and the diameter of the circular slot stub, located behind the coaxial feed location, as shown in figure - in section 2.4. Width is calculated to be one half of the minimum wavelength of operation, and length is calculated to be the minimum wavelength of operation. The diameter of the slot stub is calculated to be one fourth of the effective wavelength. Another vital specification is the exponential curve of the sides of the tapered slot, which is calculated in section 2.4.

Currently, two versions of the antennas have been constructed. The first version was cut by hand primarily using tin snips, and was lacking the slot stub component. This, after testing was completed, was shown to

be unusable as an antenna. The primary reason for failure is due to the warping of the metal during hand-cutting. Because excess force was necessary for cutting, the sides of the antenna were no longer completely coplanar, causing the gap to no longer have a consistently changing width. If the width of the slotline does not expand consistently, then crippling impedance ruins the antenna. The second version of the antenna looked to resolve this issue by having it cut in the mill of the EIC building. Machine-cut antennas not only keep the antenna completely flat, but also create a much smoother exponential curve in the expanding slotline, making impedance transition much less of an issue. The primary issue with this version was that, due to miscommunication and lack of experience, the antennas were cut from aluminum, making soldering to the surface of the antenna nigh impossible. A picture of both antenna versions can be seen in figure 4.2.



Figure 4.2: Vivaldi Antenna Version 1 (above), and Version 2 (below)

The RF chokes being used as baluns in this project is simple in design, but its large design can prove to be cumbersome in the future. Therefore, a transition from an RF choke to a balun that can be printed to a PCB is recommended for the future. One of the RF chokes being used in this system can be seen below in figure 4.3.



Figure 4.3: RF Choke

The cables chosen to be used for the balun are two 5-ft 50 ohm RG58 SMA male/SMA female cables, wrapped around 60 cm diameter toroid cores with an inductance factor of 7.16 microHenrys. The cables to be soldered to the antennas are two 5 cm long SMA female to open cable. The second version of the antennas was created using SOLIDWORKS, and the drawing of the design is attached below in Appendix B.

Table 4.1
Antenna Specification Compliance Matrix

Specification	Min	Nominal	Max
Operating Frequency	2.4025 GHz	N/A	2.4775 GHz
Length of Tapered Slot	.125 m	.126 m	N/A
Width of Tapered Slot	.0625 m	.0635 m	N/A
Diameter of Circular Slot Stub	.0306 m	.0306 m	.0306 m

4.4 Subsystem Challenges and Solutions

A big challenge for this subsystem was figuring out the design of a coplanar antenna without the use of a standard insulating substrate, such as FR4. The reason this is an issue is because I could not find any previous examples where this was done through my research. After realizing that a higher dielectric constant in the substrate lead to a smaller necessary slotline gap width, I calculated that a width of about 1 mm was needed. This, along with keeping the antenna flat after construction, was the primary reason for the difficulties that came with antenna version 1. Both issues were resolved when the second vivaldi

Daniel Miller, Tyler Castro, Michael Turner, Coy Coburn

antenna was planned using SOLIDWORKS. The EIC milling machine was able to get to a gap width of 46 mils, which is 1.1684 mm.

The unforeseen issue that arose with the development of version 2 was its aluminum material. Although difficult, I was able to establish a rather weak connection to version 1 using the EIC's standard soldering materials, but tried fruitlessly for weeks with version 2, thinking it was steel. Aluminum not only instantly oxidizes in air, but aluminum oxide is also not easily removed by normal flux. In order to create this connection, I would need to perform the soldering in a controlled environment lacking oxygen, which was never able to be done. The easiest solution would be to purchase my own copper sheet metal and move on to version 3.

4.5 Subsystem Technical Details

A diagram of the vivaldi antenna is shown in (2.1). Note that instead of a microstrip feedline, we are soldering the conductors of a coaxial cable directly to the feed point shown in the diagram. The purpose of using a vivaldi antenna is to provide a smooth transition between the wave being guided through the slotline to the plane wave. This is made possible through the exponential curve of the slotline. The coaxial cable is soldered to where the voltage difference occurs across the slotline gap. As the signal travels across the edges, the increase in the size of the gap causes a gradual change in impedance, until the signal is matched with its surrounding medium, allowing it to propagate out of the metal. The coordinates for the curve are found using (2.1), with (2.2) and (2.3) being supplemental. The coordinate system used has the origin at the center of the coaxial feed point. This mean that, for one side of the antenna and with an initial slotline width of 2 mm, $(z_1, y_1) = (0, 1)$ and $(z_2, y_2) = (126, 31.75)$. The rate of expansion, R , should be adjusted according to how the antenna performs during testing, but as a starting point, has been set to .2 after consulting other vivaldi antenna tests. This sets C_1 at .220561 and C_2 at -.263939, making the equation used for the curvature of our antenna (2.4).

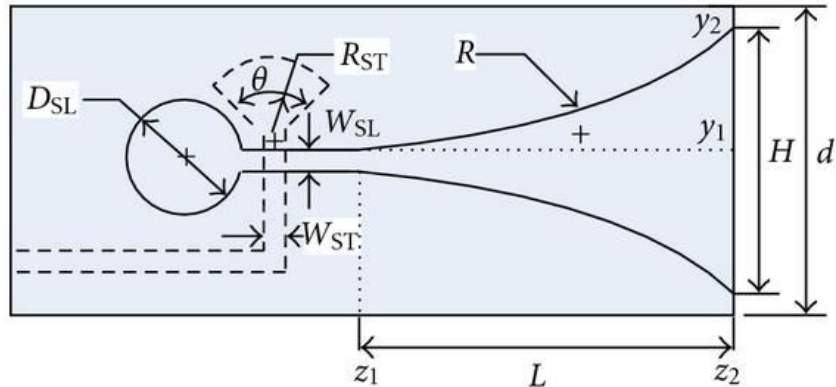


Figure 4.4: Vivaldi Antenna Diagram, with microstrip feedline

$$z = C_1 e^{Ry} + C_2 \quad (4.1)$$

$$C_1 = \frac{(z_2 - z_1)}{(e^{Ry_2} - e^{Ry_1})} \quad (4.2)$$

$$C_2 = \frac{(z_1 e^{Ry_2} - z_2 e^{Ry_1})}{(e^{Ry_2} - e^{Ry_1})} \quad (4.3)$$

$$z = .220561e^{.2y} - .263939 \quad (4.4)$$

The balun is a vital aspect of the antenna system, as directly soldering an unbalanced line such as a coaxial cable to a balanced antenna has debilitating effects. Common mode waves, where current is flowing in the same direction on both conductors of the transmission line, is undesirable because it causes the outer surface of the coaxial cable to radiate, causing power to be lost radiating in the wrong direction, which makes the antenna much less effective. For our subsystem, an RF choke balun is to be implemented using a toroidal core. Before feeding into the antenna, the coaxial cable will be wrapped around the toroidal core N amount of times, preventing signals from flowing along the outer surface of the coaxial cable. The necessary amount of loops around the core, N, is expected to be 10, but can be modified if performance is not acceptable.

Vivaldi antennas generally have a gain of roughly 5-10 dBi, and we are expecting a bandwidth of about 75 MHz. The reflection coefficient at the input, S_{11} , is expected to be around .333, and is dependent on how smooth and sharp the exponential curve of the antenna is.

Table 4.2
Antenna Design

Parameter	Specification	Simulation Results
Gain	5-10 dBi	-
Bandwidth	75 MHz	-
Reflection Coefficient	.333	-

4.6 Subsystem Testing

4.6.1 Testing of Antenna Version 1

The purpose of this test is to use a network analyzer to fully test the functionality of the constructed vivaldi antennas in order to verify that the specifications allow the antenna to operate at an acceptable level for the system as a whole. The major passing condition is whether the antenna is deemed able to properly emit a signal powerful enough to overcome attenuation through the ground, as well as have a low enough reflection coefficient to allow propagation. Properties of the antenna being tested cannot easily be altered after construction, so testing can only be performed once before another antenna must be constructed.

Test Setup

The input coaxial line will be fed into a network analyzer for testing. A special cable (N-type male to SMA male) was used for the balun in order to have the system be able to connect to the network analyzer. The network analyzer needs to be properly calibrated before use. The vivaldi antenna must be facing free space with no obscurities around it. The primary results to be analyzed from the network analyzer include the reflection, the VSWR, the smith chart, and the radiation.

Data

# Version 1.00		
#		
# Ref Impedances: Z01: 50	Z02: 50	
#		
freq[Hz]	db:Trc2_S11	ang:Trc2_S11
2.40E+09	-7.08E-01	1.08E+02
2.40E+09	-6.75E-01	1.09E+02
2.40E+09	-6.58E-01	1.09E+02
2.40E+09	-6.64E-01	1.09E+02
2.41E+09	-6.87E-01	1.09E+02
2.41E+09	-7.30E-01	1.08E+02
2.41E+09	-7.87E-01	1.07E+02
2.41E+09	-8.51E-01	1.06E+02
2.42E+09	-9.18E-01	1.05E+02
2.42E+09	-9.75E-01	1.03E+02
2.42E+09	-1.02E+00	1.02E+02
2.42E+09	-1.04E+00	1.00E+02
2.43E+09	-1.04E+00	9.90E+01
2.43E+09	-1.02E+00	9.79E+01

Team 24 Ground Penetrating Radar

2.43E+09	-9.73E-01	9.71E+01
2.43E+09	-9.18E-01	9.66E+01
2.44E+09	-8.54E-01	9.65E+01
2.44E+09	-7.88E-01	9.66E+01
2.44E+09	-7.30E-01	9.69E+01
2.44E+09	-6.82E-01	9.74E+01
2.45E+09	-6.48E-01	9.79E+01
2.45E+09	-6.33E-01	9.83E+01
2.45E+09	-6.39E-01	9.86E+01
2.45E+09	-6.65E-01	9.87E+01
2.46E+09	-7.10E-01	9.85E+01
2.46E+09	-7.71E-01	9.80E+01
2.46E+09	-8.41E-01	9.72E+01
2.46E+09	-9.15E-01	9.61E+01
2.47E+09	-9.84E-01	9.48E+01
2.47E+09	-1.04E+00	9.34E+01
2.47E+09	-1.07E+00	9.19E+01
2.47E+09	-1.09E+00	9.06E+01
2.48E+09	-1.08E+00	8.94E+01
2.48E+09	-1.04E+00	8.85E+01
2.48E+09	-9.92E-01	8.79E+01
2.48E+09	-9.30E-01	8.75E+01
2.49E+09	-8.65E-01	8.75E+01

Daniel Miller, Tyler Castro, Michael Turner, Coy Coburn

2.49E+09	-8.00E-01	8.77E+01
2.49E+09	-7.46E-01	8.80E+01
2.49E+09	-7.04E-01	8.84E+01
2.50E+09	-6.79E-01	8.88E+01
2.50E+09	-6.75E-01	8.91E+01
2.50E+09	-6.93E-01	8.92E+01
2.50E+09	-7.30E-01	8.91E+01

Test Conclusion

The results of the version 1 testing revealed almost complete reflection of the incoming signal. Even a moderate reflection of the signal should be taken as a failure, but reflection of this scale indicates that cutting by hand is not a viable option for antenna construction at all. The amount of reflection also prohibited the test from revealing the gain of the antenna as well. The results of this test are the primary reason for moving on to version 2.

4.6.2 Testing of Antenna Version 2

The purpose of this test is to use a network analyzer to fully test the functionality of the second version of the vivaldi antennas in order to verify that the specifications allow the antenna to operate at an acceptable level for the system as a whole. The major passing condition is whether the antenna is deemed able to properly emit a signal powerful enough to overcome attenuation through the ground, as well as have a low enough reflection coefficient to allow propagation. Properties of the antenna being tested cannot easily be altered after construction, so testing can only be performed once before another antenna must be constructed.

Test Setup

The setup for this test is identical to the previous test. A special cable (N-type male to SMA male) was used for the balun in order to have the system be able to connect to the network analyzer. The network analyzer needs to be properly calibrated before use. The vivaldi antenna must be facing free space with no obscurities around it. The primary results to be analyzed from the network analyzer include the reflection, the VSWR, the smith chart, and the radiation.

Data

Currently, the test has not yet been completed because of the difficulties soldering from its aluminum design. A third version with a copper material should be constructed next year for superior antenna gain and ease of connection.

Test Conclusion

Currently, the test has not yet been completed because of the difficulties soldering from its aluminum

Daniel Miller, Tyler Castro, Michael Turner, Coy Coburn

Team 24 Ground Penetrating Radar

design. A third version with a copper material should be constructed next year for superior antenna gain and ease of connection.

Daniel Miller, Tyler Castro, Michael Turner, Coy Coburn

5 Subsystem LNA and Receiver Protection

The receiving circuit will take the signal obtained by the receiver antenna and amplify the signal before passing it on the mixer. Circuit itself will consist of a schottky diode clamp and an LNA (Low Noise Amplifier). Figure 5.1 is the circuit diagram of the subsystem.

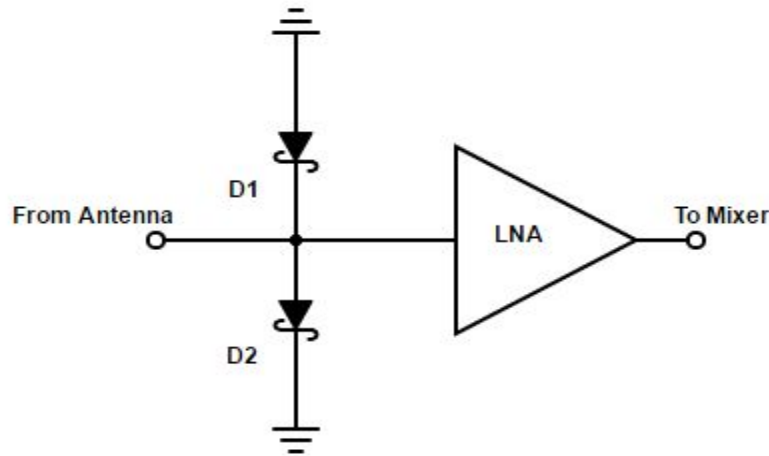


Figure 5.1: Receiver Circuit Diagram

5.2 Significant Changes in Direction

The original design of the circuit consisted of a TVG (Time Varying Gain) followed by a LNA. The TVG was removed due to the risk of it producing noise that could lead to the loss of detected objects. A PIN diode and a schottky diode clamp were added to help prevent high powered signals, that could be generated from the air to ground reflection, from damaging the LNA. A driver was added to control the switching of the PIN diode. Later the PIN diode and its driver circuit were removed do to the complexity of the driver circuit, the preferred switching time of 1ns was unable to be obtained . These changes help simplify the design and construction of the receiver circuit as well as help improve its ability to handle the signal obtained by the receiver antennas.

5.3 Subsystem Status

In order to prepare the signal for converting, the receiver circuit must be able to amplify the signal for the mixer while limiting the power of the incoming signal to protect the LNA. The LNA that was chosen had to work in the frequency range while having as low of a noise figure as possible. The schottky was chosen to have a forward voltage between the LNAs input compression point and its maximum input power. The Table 5.1 list the components and the important specifications of each.

Table 5.1
Receiver Circuit specification Compliance Matrix

Specification	Min	Nominal	Max
LNA Frequency Range	0.05 GHz	--	4 GHz
LNA Gain	10.2 dB	12.5 dB	13.3 dB
LNA Noise Figure	0.98 dB	1 dB	1.10 dB
LNA Output Power @ 1dB compression	19.8 dBm	20.7 dBm	21.2 dBm
LNA max input power	--	--	17 dBm
LNA DC Voltage	3 V	5 V	6 V
LNA DC Current	33 mA	58 mA	76 mA
Schottky Diode Forward Voltage	250 mV	340 mV	700mV
Schottky Diode Capacitance	--	1 pF	--

5.4 Subsystem Challenges and Solutions

Major challenges include designing the PIN diode driver, constant change of the transmitting signal, the lack of breadboard prototyping, and problems purchasing the proper parts.

The PIN diode shunt switch was initially added to protect the LNA from power spikes generated from air to ground interference. A diode driver switch was to be designed to control the PIN diode switching by producing the correct forward voltage and reverse current. Research showed that the switching speed would need to be around 1ns to prevent loss of useful data. Purchasing a driver of that speed would be very expensive so designing one from scratch was the only option. Although an attempt was made to design the driver, the PIN diode was removed with the assumption that the schottky diode clamp will be enough to protect the LNA.

The initial transmitting signal was based on a pulsing design that would be timed based on a clock. The clock would have also been used to signal the switching of the PIN diode driver. However the way that transmitting signal was generated was changed and the clock was removed, cause the problem of how to time the PIN diode driver. Eventually the PIN diode drive was removed from the subsystem due to this and the time constraint.

Lack of breadboard prototyping is due to the high frequency rates that are being utilized as well as the components being mostly surface mounts and not through hole. The main method used was ADS (Advanced Design System), a RF simulator. This would have allowed for simulations to make up for the lack of breadboard usage however ADS does not have a schottky diode model built in and attempts to add one failed.

Lack of initial knowledge of RF and electrical systems led to wrongful purchase of parts such as the first LNA (TAV-541+) and the SMA surface mount connectors. The first LNA was replaced due to it requiring external biasing and not enough time to do so. The SMA surface mount connectors were replaced with through hole ones to make soldering them easier.

5.5 Subsystem Technical Details

The LNA is the main component of the receiver circuit as it is required to amplify the signal for the signal converter. The LNA needs a very low noise figure and must be able to handle the required frequency range of 2.4GHz. The CMA-5043+ was chosen because it meets the requirements with a frequency range of 0.05 GHz to 4 GHz, a noise figure of 1 dB at 2.4 Ghz, and has a gain of 12.5 dB at 2.4 Ghz.

MiniCircuits, the company that produced the LNA that was chosen, also produces an eval board for it. The TB-757+ was chosen as due to convenience and the complexity of making a PCB for the LNA from scratch. The eval board is matched to the 50Ω impedance of the entire system.

The schottky diodes are added to protect the LNA from high powered signals. Figure 5.1 shows the configuration of the two diodes. The activation range of the schottky diode was determined to be between the LNAs input compression point and its maximum input power. By choosing a schottky diode that would be fully activated within that range would guarantee that it would protect the LNA from damage while obtaining the full use of the LNA. Equation (5.1) was used to calculate the LNAs input compression point (P_{1db_in}) to be 7 dBm.

$$P_{1db_in} = P_{1db_out} - Gain \quad (5.1)$$

Using the dBm to RMS voltage equation (5.2), it was calculated that the schottky must have a forward voltage greater than 0.5 V but lower 1.5V. The 1PS70SB82_84_85_86 series was chosen because it meets the requirements with a max forward voltage of 0.7 V.

$$Voltage = \sqrt{(50\Omega * 1dBm) * 10^{power/10}} \quad (5.2)$$

The 1PS70SB82_84_85_86 series is a double diode consisting of 4 different configurations. 1PS70SB84 package was chosen due to the layout of the diodes being in-line as shown in Figure 5.2.

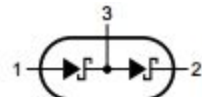


Figure 5.2: Schottky diode configuration

When designing the PCB for the schottky diodes, the trace width (W) had to be large enough to be a 50Ω microstrip. This calculation is based on the thickness of the copper trace (T), the thickness of the PCB dielectric (H), the relative permittivity of the dielectric (ϵ_r), and impedance (Z_0) we want the trace to match too. Equation (5.3) was used to calculate the trace width to be 110 mils to have an impedance of 50Ω .

$$Z_0 = \frac{87}{\sqrt{\epsilon_r+1.41}} \ln \left(\frac{5.98 * H}{0.8 * W + T} \right) \quad (5.3)$$

5.6 Subsystem Testing

Two test will be performed for the receiver circuit. The first will test if the schottky diodes can limit high powered signals that can damage the LNA. The second will test if LNA works properly and will amplify the signal enough to drive the mixer.

5.6.1 Schottky Diodes

The purpose of this test it to determine if the Schottky diodes can protect the LNA from high powered signals. The Schottky needs to turn on when the input is between 7 dBm and 17 dBm to sufficiently prevent high powered signals from passing to the LNA. The test will pass if the Schottky diodes can activated within that range.

Test Setup

The test will be conducted in lab using the network analyzer and the schottky diode PCB. The network analyzer will run a power sweep from 1 dbm to 20 dBm with a frequency of 2.4 GHz. The sweeping range was chosen to be outside the required range that the schottky diodes need to activate at.

Data

No data is available for this section.

Conclusion

Theoretically the Schottky should operate in according with the data sheet and properly protect the LNA. Since network analyzer wasn't easily available and the N-type to SMA cables needed to test the system could not be purchased in time, no testing was ever done.

5.6.2 LNA

The purpose of this test it to determine if the LNA can properly increase the received signal large enough to drive the mixer. The test will pass if the LNA can properly do that.

Test Setup

The test will be conducted in lab using the network analyzer and the LNA eval board. The network analyzer will be used to test gain generated by the LNA.

Data

No data is available for this section.

Conclusion

Theoretically the Schottky should operate in according with the data sheet and properly protect the LNA. Since network analyzer wasn't easily available and the N-type to SMA cables needed to test the system could not be purchased in time, no testing was ever done.

6 Subsystem Receiver Converter

The purpose of the receiver signal converter subsystem is to take the Rx signal and convert its wave into digital points to be used for image processing. Once the received signal has been amplified by the LNA circuit, it will then be sent through a frequency mixer to manipulate the frequency back to the frequency that was originally transmitted. A DDS will be used as the LO feed for correct matching. Once mixed, the resulting IF signal is fed to a demodulator and ADC to sample and convert the analog signal into digital values that will be recorded and saved for image processing uses.

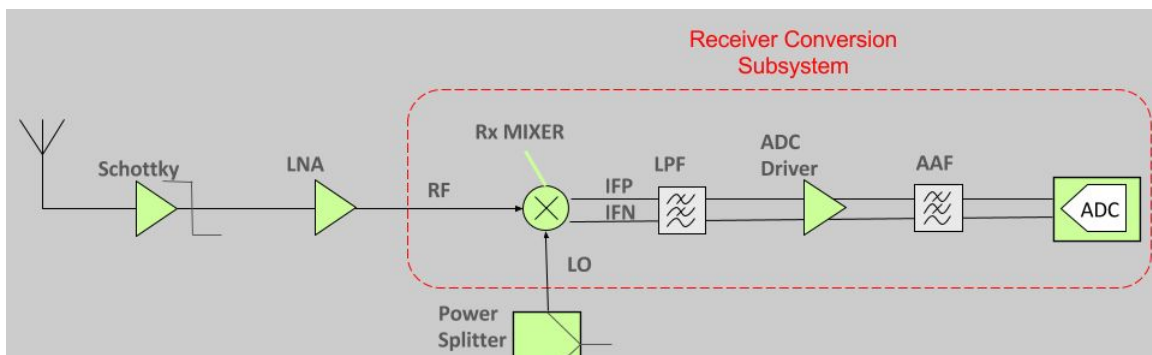


Figure 6.1 Receiver Converter Block Diagram

6.2 Significant Changes in Direction

Multiple changes have been made during the production of this subsystem. Originally, a BeagleBone Black was chosen for AD conversion, however the sampling rate of a regular unit is 200 KHz, which is too low for the necessary sampling frequency needed for this circuit. Earlier requirements included processing the digital data into an image displayed on screen for the user, however the new requirement is to only record and store the digital data into easily imported files for other machines and systems to use. Finally, the phased array portion of the project was replaced with only one channel. This resulted in the circuit's need of only one mixer instead of a mixer for each channel and power combiner. The coaxial phase shifters were also removed from the subsystem due to this change.

The subsystem itself has also gradually increased size as well. Based on a Heterodyne architecture, the blocks grew to include a mixer, LO input from the transmitter's power splitter, a LPF, ADC driver, AAF, and ADC plus evaluation equipment.

6.3 Subsystem Status

The mixer, LPF, and AAF have been completed. The ADC driver's evaluation board needs completion and testing. The ADC itself depends solely on time and cost restraints. While two different chips have been received, the massive sampling rates these ADC's possess results in the need of a FPGA data configuration kit. Analog Devices sell this equipment, however it can be costly. Visual Analog is the software chosen for

digital data manipulation. It is intended to operate the data capture board and can also model image processing.

Table 6.1
Receiver Converter specification Compliance Matrix

Specification	Min	Nominal	Max
RF Frequency Range	2.415 GHz	--	2.420 GHz
RF gain level	-20 dBm	-15 dBm	-13 dBm
LO Frequency Range	2.415 GHz	--	2.420 GHz
IFP and IFN Frequency	0 Hz	194 kHz	10 MHz
LPF gain	--	3.0 dB	--
LPF/AAF cutoff frequency	--	264 kHz	--
AAF gain	--	1.5 dB	--
ADC sampling rate	> 20 Msps	32 Msps	< 60 Msps
ADC operating voltage	2.7 V	--	5.5 V

6.4 Subsystem Challenges and Solutions

Major challenges include the dependence on RF and LO signals, the high cost for parts including mixer, power splitter, and ADC, the lack of breadboard prototyping, and finding the necessary processor to handle high-speed ADC sampling rates.

According to calculations, the expected IF signal generated will be about 194 - 200 kHz. This number can differ due to the RF and LO frequency rise and fall overlap. In worst case scenarios, the actual bandwidth of 10 Mhz can be found. However, increasing the triangular wave fall time from the original idea of a sawtooth wave at the transmitter should prevent this scenario from occurring.

The high cost of the parts needed is probably one of the harder obstacles to avoid. In earlier designs, a DDS would be used as the LO input. This was eventually replaced with a power splitter to send the Tx signal to the mixer instead, reducing cost to \$60 instead of \$800. Other methods include buying bareboards for the device chips and populating them with the necessary components from the given datasheets. This was conducted for the ADC driver and filtering stages of the subsystem. More complex diagrams, like the ADC or possibly the mixer, should buy from the manufacturer.

Lack of breadboard prototyping is due to the high frequency rates that are being utilized as well as switching from eval boards with sma outputs. The main method used was Advanced Design System, a RF simulator received from the professor and installed onto certain terminals in the Weisenbaker building. This allowed for simulations to make up for the lack of breadboard usage.

Contact was made with a representative and field applications engineer from Analog Devices. This engineer recommended certain equipment as well as began process to lend ADC equipment. However, this did not come in time for simulations but might be a path for future process to be made.

6.5 Subsystem Technical Details

The mixer is fundamental in correcting any frequency change occurs in the received signal. The mixer needs to be able to work in the bandwidth range expected. In this project, 2.415 - 2.420 GHz is the expected range. The LO power into a diode mixer should be 10 dB greater than the highest input signal level anticipated. Calculations lead to an expectation of -28.16 dBm to be the received power. With LNA amplification, this number can be increased to -15.16 dBm. This will meet requirements with a LO power of -5 dBm at minimum. However, high-IP3 mixers can work with a LO power 3dB less than the RF power. The 1-dB compression point is used for choosing the mixer's LO power. The receiver power (P_r) is found from the factors of transmitted power (P_t), antenna gain (G), radar cross section (σ), transmit wavelength (λ), and range (R) as shown in equation 6.1.

$$P_r = \frac{P_t G^2 \sigma \lambda^2}{(4\pi)^3 R^4} \quad (6.1)$$

The expected IF to be mixed is based on LO - RF and LO + RF at a specific time. With the sweeping frequency, the IF can also change. The IF can be calculated from the bandwidth (fbw), range (R), time of flight (T), and speed through the sand medium (v_{sand}) as shown in equation 6.2. This leads to the expected 194 kHz. The outputs are differential; this provides noise immunity as well as a cancellation on even-order harmonics.

$$f_B = \frac{2f_{BW}R}{v_{sand}T} \quad (6.2)$$

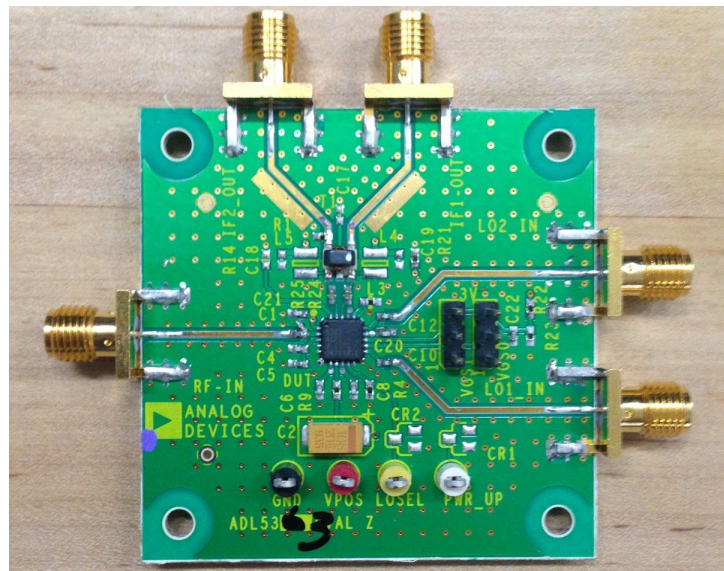


Figure 6.2: Frequency Mixer with eval board

Table 6.2
Mixer design

Parameter	Specification	Simulation Results
RF frequency	2.415 - 2.420 GHz	2.415 - 2.420 GHz
LO frequency	2.415 - 2.420 GHz	2.415 - 2.420 GHz
IF frequency	194 kHz	0 - 203 kHz
Received power	-28.16 dBm	N/A

The LPF and AAF filtering stages were built onto one PCB. A low pass filter is utilized to attenuate the up converted IF while allowing the down converted IF to pass through. The filter consists of a two 1st order butterworth filters in series. The 250 Hz cutoff frequency prevents the up conversion image to pass, but also to protect from any unexpected IF spikes. The AAF continues this trend to ensure the signals are in the needed range after passing through the ADC driver. LT8138 op amps were chosen for their high GBWP which allows for any changes needed in amplifying or attenuating voltage gain.

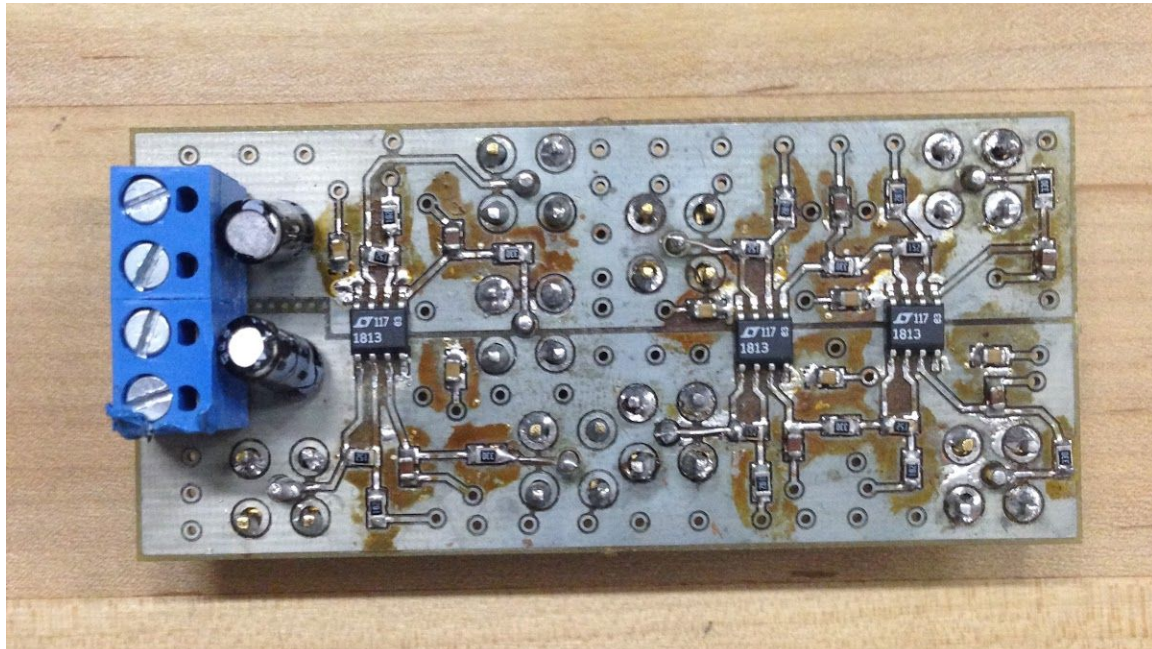


Figure 6.3 Low pass filter and Anti-alias filter stages

Table 6.3
Low pass filter design

Parameter	Specification	Simulation Results
Gain	3.0 dB	2.8 dB
Bandwidth	250 kHz	264 kHz

Daniel Miller, Tyler Castro, Michael Turner, Coy Coburn

GBWP	< 100 MHz	28 MHz
Order	2nd	2nd

Table 6.4
Anti-alias filter design

Parameter	Specification	Simulation Results
Gain	1.5 dB	1.4 dB
Bandwidth	250 kHz	264 kHz
GBWP	< 100 MHz	29 MHz
Order	1st	1st

The ADC driver is utilized as a buffer and voltage amp before the IFP and IFN are sent to the ADC board. Depending on the ADC chosen, the voltage ranges must be in either the 2.7 - 5.5 V range or else the 2.1 - 5.5 V range.

The ADC is the final piece of hardware in the subsystem and GPR system as a whole. The ADC takes samples of the incoming analog signals and converts them to a digital signal based on the bit resolution. The AD9280 has a 8 bit resolution which means that there are 256 different voltage levels that can be obtained from the incoming signal. Most importantly, a high sampling rate is needed for proper digital conversion. Based on Nyquist theorem, sampling rate($f_{sampling}$) must be greater than twice the nyquist frequency (BW) which is the bandwidth in worst case scenarios. The frequency resolution is found from the spatial resolution, speed through sand, and bandwidth over the rise time (T_r) as shown in equations 6.6 to 6.9. The ADC chosen has a sampling rate of 32 Msps, which meets these requirements. However, a FPGA configuration board is needed to process this massive amount of data being converted. The HSC-ADC-EVALCZ has been chosen for this requirement.

$$f_{sampling} = 2 * BW \quad 6.6$$

$$\Delta f = \frac{2 * spatial\ resolution}{C_{sand}} * \frac{BW}{T_r} \quad 6.7$$

$$\Delta f = 1/T \quad 6.8$$

$$T = \frac{samples}{f_{sampling}} \quad 6.9$$

Table 6.5 ADC design

Parameter	Specification	Simulation Results
Sampling rate	> 10 Msps	32 Msps
Resolution	8 bits	8 bits

Daniel Miller, Tyler Castro, Michael Turner, Coy Coburn

Resolution frequency	1.2 Hz	1.27 Hz
Voltage diff level	0.011 V	0.017 V

6.6 Subsystem Testing

Give a summary of the important testing here, followed by the test plans (in order). An example of the structure of a test plan is shown below.

6.6.1 Mixer IF output test

The purpose of this test is to view and analyze the IFP and IFN outputs from the frequency mixer. Wanted results included a down converted signal of 200 kHz as well as a up converted signal of 4.83 Ghz.

Test Setup

The test setup includes using a network analyzer with two channels; a RF and LO channel of sweeping frequency 2.415-2.415. The RF sweep must be offset by 20 ns, which is the expected time of flight for the RF to return to the receiver antenna. A spectrum analyzer will be utilized to view the differential outputs from the mixer.

Data

No data is available for this section

Conclusion

Theoretically the mixer board should operate in according with the data sheet and properly mix the incoming signals to the IFP and IFN outputs. R1 on the actual eval board needs to be removed to change from single-ended to differential output as well.. Since network analyzer wasn't easily available and the N-type to SMA cables needed to test the system could not be purchased in time, no testing was ever done.

6.6.2 Filtering Stages Test

The purpose of this test is to filter the IFP and IFN stages and amplify their voltage gains.

Test Setup

The test setup includes using the frequency mixer's test setup. The RF sweep must be offset by 20 ns, which is the expected time of flight for the RF to return to the receiver antenna. Instead of connecting to the spectrum analyzer the outputs will be sent through the LPF stage for up conversion rejection. A spectrum analyzer will be utilized to view the differential outputs from the LPF. Once this test has proven positive, the second phase will include passing through the ADC driver board and through the AAF stage. Same expectations will be held here and validated by analyzing the spectrum analyzer.

Data

No data is available for this section

Daniel Miller, Tyler Castro, Michael Turner, Coy Coburn

Conclusion

Theoretically the low pass filter and anti-alias stages should operate in accordance with the simulations and properly filter the incoming signals. Since network analyzer wasn't easily available and the N-type to SMA cables needed to test the system could not be purchased in time, no testing was ever done.

7 Conclusions

This document illustrates the progress made in the creation of a Ground Penetrating Radar as well as the necessary research and understanding needed to design and implement all subsystems. Each subsystem is close to proper functioning but still needs further testing. The most difficult process of this project is the integration of all the subsystems as well as the testing of the whole system itself. As the transmitted signal is not only sent to the antennas for signal propagation, but also to the LO input as reference for the returning signal. Therefore, the transmission must be in range, the medium's dielectric constant must be in range for the device, and the antennas must be able to fully transmit and receive in the frequency range.

PCB boards were only made in the last couple of weeks during this project. This slowed testing progress and limited updates and redesigns to PCBs. Recommendation would be to create new PCBs every 2 weeks for further testing as well as improvement in design. Necessary RF equipment for testing purposes proved to be difficult to acquire. Recommendation would be to seek equipment from Texas A&M staff and researchers to lend, with an early contract and tutorials to ensure proper usage and easy access. Continue to use ADS for early simulations and begin with tutorials before actual GPR project. RF mentors are a highly helpful source but in short supply. Recommend to contact RF engineer and create strong connection during designing process. Also recommend to ask for RF engineer as teacher assistant for project as well.

While unable to completely reach our intended results, each subsystem has been calculated and established in accordance with our simulations. Our work this semester provides a solid foundation for the next team who decides to continue this project. Continuing on, additional improvements can be made to each subsystem, integration needs to be completed, housing for components needs to be created, and additional parts are needed to process the samples (ADC and FPGA).

References

References should be included as per the IEEE format.

- [1] Christian Wolff, "Phased Array Antenna ,," [Online]. Available at: <http://www.radartutorial.eu/06.antennas/Phased%20Array%20Antenna.en.html>. [Accessed: 2015]
- [2] Cedric Martel, "Modelling and Design of Antennas for Ground-Penetrating Radar Systems ,," Ph.D. dissertation, Dept. Elect. Eng, Univ. of Surrey, Guildford, United Kingdom, 2002.
- [3] "Ground Penetrating RADAR (GPR) (After Basson 2000) Introduction," GPR theory, 2007. [Online]. Available at: <http://www.geo-sense.com/gprmore.htm>. [Accessed: Jan-2015].
- [4] *Standard Guide for Using the Surface Ground Penetrating Radar Method for Subsurface Investigation*, Active Standard ASTM D6432, 2011
- [5] A. P. Annan, "Ground Penetrating Radar Principles, Procedures & Applications," Sensors & software Inc., Mississauga, Ontario, 2003
- [6] Bart Scheers, "Ultra-Wideband Ground Penetrating Radar, with Application to the Detection of Anti Personnel Landmines," Ph.D. dissertation, Dept. Elect. Eng, Catholic Univ. of Louvain, Louvain-la-Neuve, Belgium, 2001.
- [7] C. Allen , "Radar Pulse Compression ,," 2004. [Online]. Available at: https://www.ittc.ku.edu/workshops/Summer2004Lectures/Radar_Pulse_Compression.pdf. [Accessed: 2015]
- [8] Cedric Martel, "Modelling and Design of Antennas for Ground-Penetrating Radar Systems ,," Ph.D. dissertation, Dept. Elect. Eng, Univ. of Surrey, Guildford, United Kingdom, 2002.
- [9] "Ground Penetrating RADAR (GPR) (After Basson 2000) Introduction," GPR theory, 2007. [Online]. Available at: <http://www.geo-sense.com/gprmore.htm>. [Accessed: Jan-2015].
- [10] *Standard Guide for Using the Surface Ground Penetrating Radar Method for Subsurface Investigation*, Active Standard ASTM D6432, 2011
- [11] A. P. Annan, "Ground Penetrating Radar Principles, Procedures & Applications," Sensors & software Inc., Mississauga, Ontario, 2003
- [12] Bart Scheers, "Ultra-Wideband Ground Penetrating Radar, with Application to the Detection of Anti Personnel Landmines," Ph.D. dissertation, Dept. Elect. Eng, Catholic Univ. of Louvain, Louvain-la-Neuve, Belgium, 2001.

Daniel Miller, Tyler Castro, Michael Turner, Coy Coburn

Appendix A Budget Table

Include a table listing the purchases/expenses for the project thus far, and note any known pending expenses.

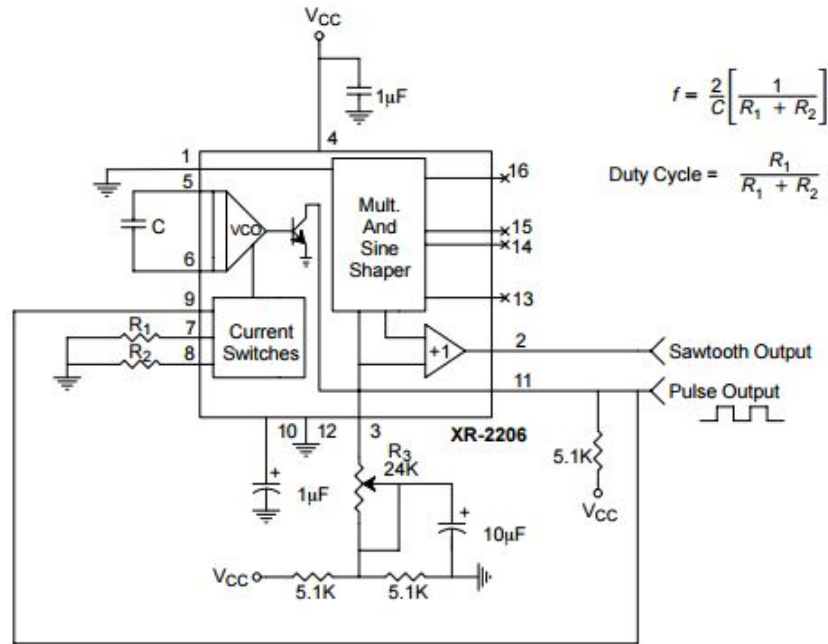
Table A-1: Project Budget

Description	Quantity	Item Cost	Shipping	Subtotal
XR-2206 (Function Generator)	2	7.95	6.63	22.53
PA	2	10.86	15.95	40.78
VCO	1	44.95	11.69	61.31
FERRITE CORE TOROID 7.16UH T37	2	24.34		24.34
CABLE SMA F JACK-STRIP/TIN 3/3MM	2	18.74		18.74
CA SMA M/SMA F RG58C/U 5'	2	28.20	11.99	42.52
CMA-5043+ (LNA)	20	1.390		27.80
TB-757+ (LNA Eval Board)	1	75		75
1PS70SB84 (Schottky diodes)	20	0.358		7.16
SMA Female PCB Mount	12	1.64		19.68
SMA Cable 6 in	10	10.148		101.48
ADC	1	9		9
ADC Driver	1	12.5		12.5
Frequency Mixer	1	6		6
Frequency Mixer Eval	1	99		99
100 MHz GBWP Op amps	3	5.17		15.5
Power Splitter	1	50		50
			Total	572.03

Appendix B

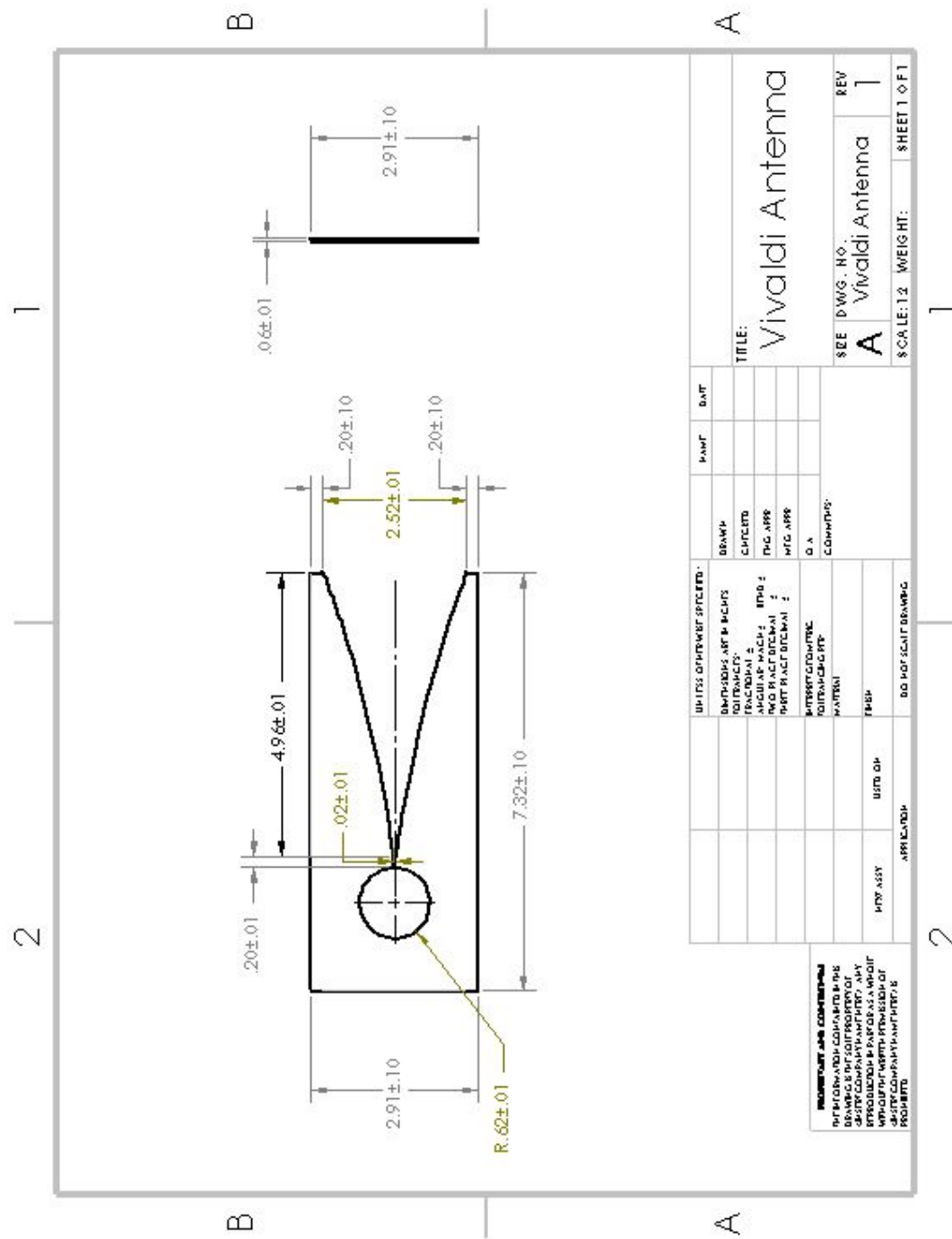
Subsystem Schematic and BOM

B-1 Function Generator Circuit

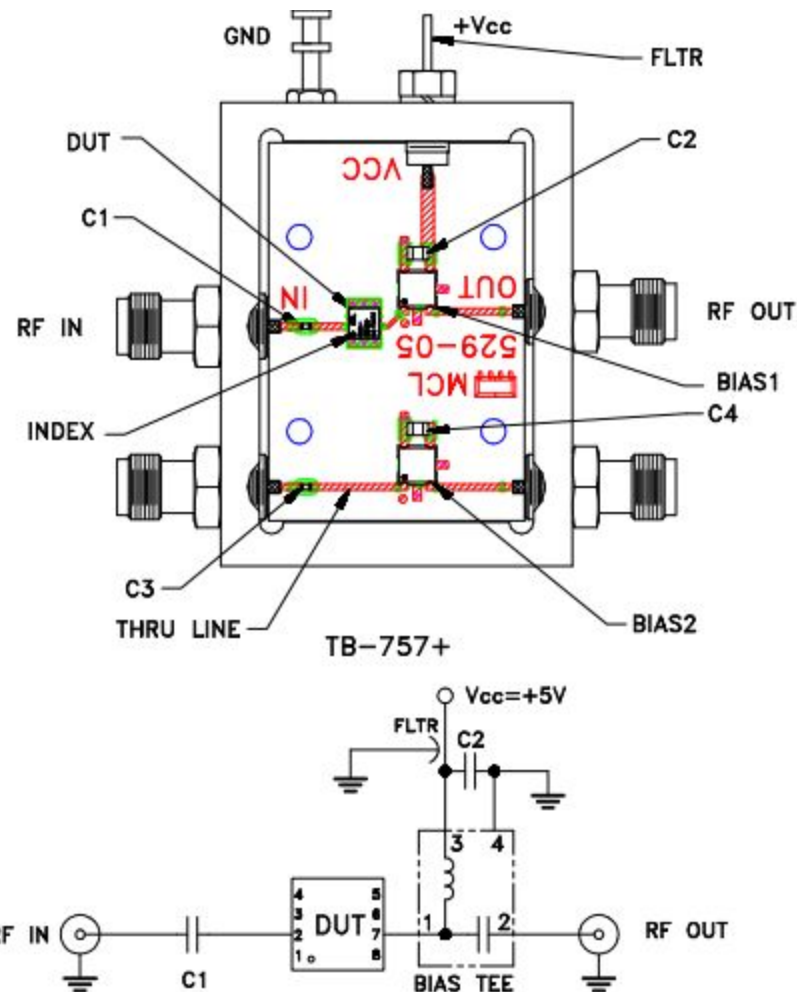


Symbol	Value	Description
C	.47uF	CAPACITOR, American symbol
R1	100k Ω	POTENTIOMETER, American symbol
R2	100k Ω	POTENTIOMETER, American symbol
	5.1k Ω	RESISTOR, American symbol
	5.1k Ω	RESISTOR, American symbol
	5.1k Ω	RESISTOR, American symbol
	50k Ω	POTENTIOMETER, American symbol
	1 μ F	CAPACITOR, American symbol
	1 μ F	CAPACITOR, American symbol
	10 μ F	CAPACITOR, American symbol

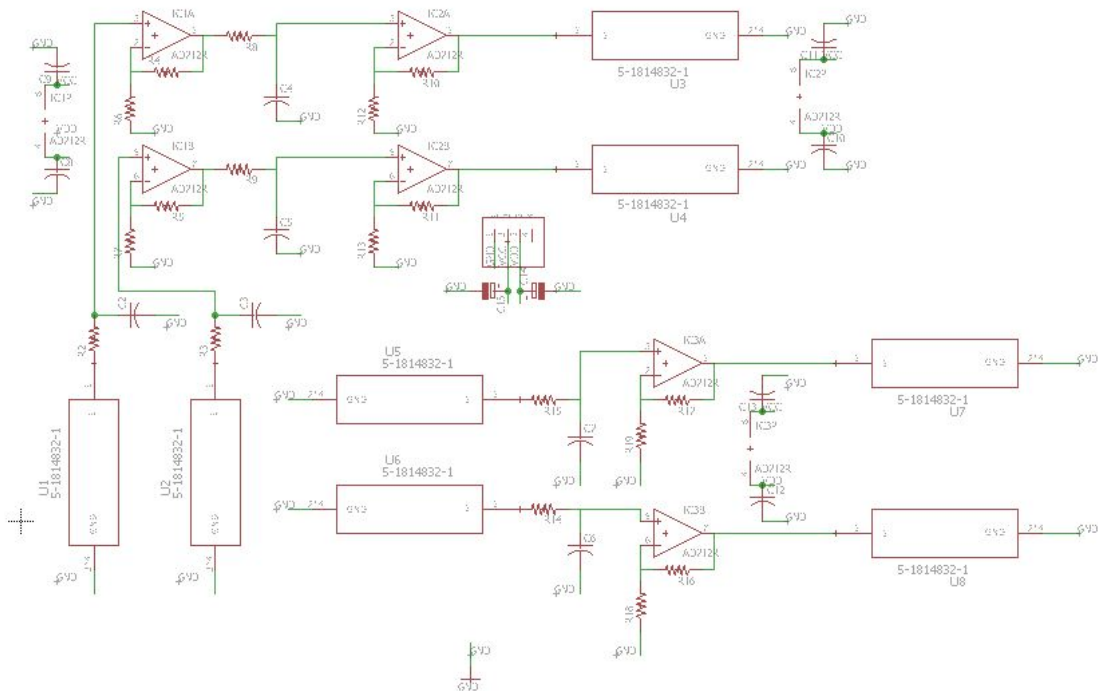
B-2 Antenna Version 2 SOLIDWORKS Drawing



B-3 LNA Eval Board Schematic



Symbol	Value	Description
DUT	CMA-5043+	LNA DUT
C1	1000 pF	CAPACITOR, American symbol
C2	0.1 uF	CAPACITOR, American symbol
FLTR	1500 pF	CAPACITOR, American symbol
BIAS TEE	TCBT-14+	MCL BIAS-TEE
RF IN/OUT		SMA Connectors

B-4 Low Pass Filter and Anti-alias Filter PCB Schematic

Symbol	Value	Description
U1 - U8		SMA PCB connector
ICxA (1 - 3)		LT8138 op amp
ICxB (1 - 3)	8-pin	LT8138 op amp
R2-3, R8-9, R14-15	33 Ω	RESISTOR, American symbol
R4-5, R10-11, R16-17	1500 Ω	RESISTOR, American symbol
R6-7, RR12-13, RR18-19	1000 Ω	RESISTOR, American symbol
C2 - C7	18 nF	CAPACITOR, American symbol
C8 - C13	0.1 μF	CAPACITOR, American symbol
C14 - C15	10 μF	CAPACITOR, American symbol